Pergamon

Journal of Structural Geology, Vol. 17, No. 1, pp. 59 to 81, 1995

0191-8141/95 $9.50+0.00

0191-8141(93)E0025-T

The case for simultaneous deformation, metamorphism and plutonism: an example from Proterozoic rocks in central Arizona

K. E. KARLSTROM

Department of Earth and Planetary Sciences, University of New Mexico, Albuquerque, NM 87131, U.S.A.

and

M. L. WILLIAMS

Department of Geology and Geography, University of Massachusetts, Amherst, MA 01003, U.S.A.

(*Received* 19 *October* 1992; *accepted in revised form* 28 *January* 1994)

Abstract—The syntectonic 1.70 Ga Crazy Basin Monzogranite provides an example of the complex spatial and temporal interactions between metamorphism, deformation, and plutonism. Synchronous plutonism and deformation is indicated by syn-shortening dikes, sills, and veins; parallel magmatic and solid state fabrics; fabrics in xenoliths; and a foliation triple point. Synchronous plutonism and metamorphism is indicated by a systematic increase from 400°C to 630°C towards the pluton at a constant pressure of 300 MPa (3 kb). Temperatures are consistent with a conductive cooling model in which a 700°C pluton was emplaced into country rocks undergoing greenschist facies regional metamorphism. Synchronous deformation and metamorphism is indicated by porphyroblast inclusion geometries that document the synmetamorphic development of the S_2 cleavage. The pluton was emplaced adjacent to the Shylock shear zone during progressive shortening. Emplacement of granite as NE-trending sheets was facilitated by temporal partitioning of transpressional convergence into strike-slip and dip-slip components. At the scale of the pluton's aureole and on the relatively rapid time scale of 10^3–10^6 y, regional deformation and metamorphism were punctuated by thermal softening and increased diffusion rates. Data suggests that accretion of Proterozoic arcs in Arizona involved diachronous pluton-enhanced deformation and associated high temperature–low pressure regional metamorphism.

INTRODUCTION

Orogenic belts are the cumulative product of deformation, metamorphism and plutonism, and syntectonic plutons offer insights into the nature and timing of interactions between these processes. In spite of recent advances in directly dating deformational and metamorphic events (Page & Bell 1985, Grambling & Ward 1987, Gromet 1991), and dating metamorphic minerals with known closure temperatures (McDougal & Harrison 1988, Zeitler 1989, Mezger *et al.* 1991), geologic studies around plutons still provide important relative and absolute timing data (Paterson & Tobisch 1988). Further, plutons have proved useful for constraining rates and durations of deformational and metamorphic processes (Karlstrom *et al.* 1993). However, in view of the many ambiguities in interpreting relative timing relationships, there is continued need for detailed documentation of timing relationships around individual plutons, and especially for studies that constrain thermal and mechanical models for emplacement of syntectonic plutons.

This paper is a case study of the interaction between deformation, metamorphism and plutonism in the Proterozoic Yavapai orogen in central Arizona. Our data indicate that the 1.70 Ga Crazy Basin Monzogranite (formally named the Crazy Basin Quartz Monzonite by Blacet (1966), and renamed here following Streickeissen (1976)) was emplaced during regional deformation and metamorphism, and the deformation, metamorphism and plutonism were intimately interrelated in time and space. Plutonism strongly influenced deformation by helping to partition strain both during and after crystallization, and metamorphism by providing heat for pluton-enhanced regional metamorphism. Thus, syntectonic plutonism focused and enhanced the deformational and metamorphic events. However, pluton emplacement itself is interpreted to have been controlled by the decoupling of dip-slip and strike-slip components of oblique convergence across a major deformation zone, the Shylock shear zone. Thus, our data emphasize the mutual interaction of syntectonic pluton emplacement and deformation partitioning.

Because regional deformation both facilitated and was itself modified by pluton enhancement, separate lines of evidence appear to support different interpretations of relative timing relationships. Numerous workers have stressed the importance of multidisciplinary approaches that use multiple criteria (Paterson & Tobisch 1988, Vernon & Flood 1988). In this study, relative timing and data are presented in terms of the three binary relationships: deformation–plutonism, plutonism–metamorphism, and metamorphism–deformation. Each binary system independently suggests synchroneity of events, but the combined tern-

ary relationships provide the strongest evidence that all three processes operated simultaneously.

Deformation–plutonism

The temporal relationship between deformation and plutonism is typically investigated by comparing deformational fabrics and structures in plutons and in adjacent country rocks to distinguish deformational fabrics that record regional strains from those that record emplacement-related strains. Interpretations of relative timing of granite emplacement and regional tectonism are complicated because of the changing rheology of granites as they crystallize (Wickham 1987, Miller *et al.* 1990), strain partitioning during deformation (Bell 1981, Page & Bell 1985, Gapais 1989), and incomplete understanding of mechanisms of pluton emplacement (Batcman 1984, Hutton 1988a, Paterson *et al.* 1991).

Plutonism–metamorphism

If plutons can be tied to some segment of the regional metamorphic *P–T* path, then constraints can also be placed on the timing or duration of metamorphism. Such temporal relationships may be critical for understanding the controls on regional metamorphism. For example, in areas such as Arizona where the distribution of metamorphic isograds is influenced by the proximity to plutons (Williams 1991), several hypotheses about the nature of regional metamorphism might be postulated: (1) plutons may cumulatively add important increments of heat to the crust (Lux *et al.* 1986, Yardley *et al.* 1987, Collins & Vernon 1991), (2) plutons may be emplaced preferentially into regional warm spots (see discussion in Brady 1988, Chamberlain & Rumble 1989), or (3) pretectonic pluton margins may affect the geometry of syntectonic isograds either by channelling metamorphic fluids and thus localizing heat, or simply by becoming hotter in the regional heat flux than the surrounding rocks (basement effect) (Ayerton 1980, Allen & Chamberlain 1989). The evaluation of these hypotheses is critically dependent on the relative timing of plutonism and metamorphism.

Metamorphism–deformation

Metamorphism and deformation each strongly influences rates and styles of the other. Deformation enhances diffusion and facilitates chemical reactions (Bell & Cuff 1989, Bell & Hayward 1991); deformation partitioning affects and is affected by porphyroblast nucleation and growth (Bell *et al.* 1986, Vernon 1989), and metamorphism may facilitate deformation through release of fluids in dehydration reactions and/or by reaction softening (Wintsch 1985, Williams 1994). Interpretations of microfabrics suggest that peak metamorphism coincides with and outlasts deformation in many orogenic belts (Bell *et al.* 1986, Vernon 1989), but a continuing challenge is to evaluate the development of metamorphic assemblages and deformational microstructures in the context of a progressive *P–T–t* history (Spear & Peacock 1989, Vernon 1989).

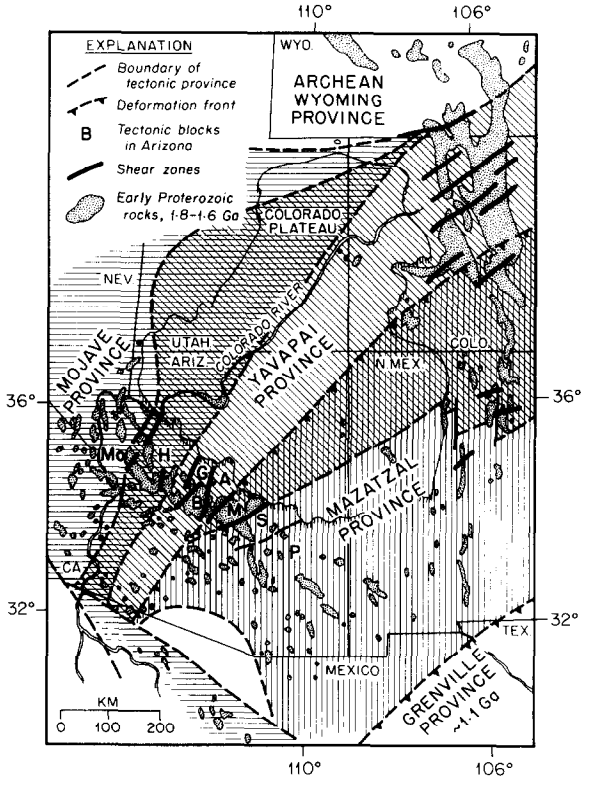

Fig. 1. Distribution of Proterozoic rocks (stipple) and tectonic provinces in the southwestern United States. The Arizona transect is divided into tectonic blocks by N- and NE-trending shear zones. Blocks are: Mo = Mojave, H = Hualapai, G = Green Gulch, B = Big Bug, A = Ash Creek, M = Mazatzal, S = Sunflower, P = Pinal. The Crazy Basin Monzogranite is located in the Big Bug block (at B), in the southeast portion of the Yavapai province. This province is characterized by juvenile arc terranes and penetrative shortening deformation at *ca* 1.7 Ga (Yavapai orogen).

GEOLOGIC BACKGROUND

Proterozoic rocks in the Transition Zone of central Arizona constitute a 500 km long cross-strike transect that is divided into a number of tectonic blocks bounded by major shear zones (Fig. 1) (Karlstrom *et al.* 1987, Karlstrom & Bowring 1988). Individual blocks with different tectonic histories are separated by shear zones that record high strain during partitioned NW–SE shortening. These high strain zones and the related regional NE-striking subvertical foliation overprint earlier fabrics and some of the shear zones apparently have early (1.70–1.74 Ga) movement histories (Bowring & Karlstrom 1990, Karlstrom & Bowring 1991, 1993). This paper deals with the relationship between the regional shortening event and the 1.70 Ga Crazy Basin Monzogranite of the Big Bug block. Although we emphasize insights about tectonic processes, our results are also important for constraining the timing of the regional shortening (Yavapai orogeny) that marked a major pulse of assembly of tectonic blocks to North America (Karlstrom & Bowring 1988).

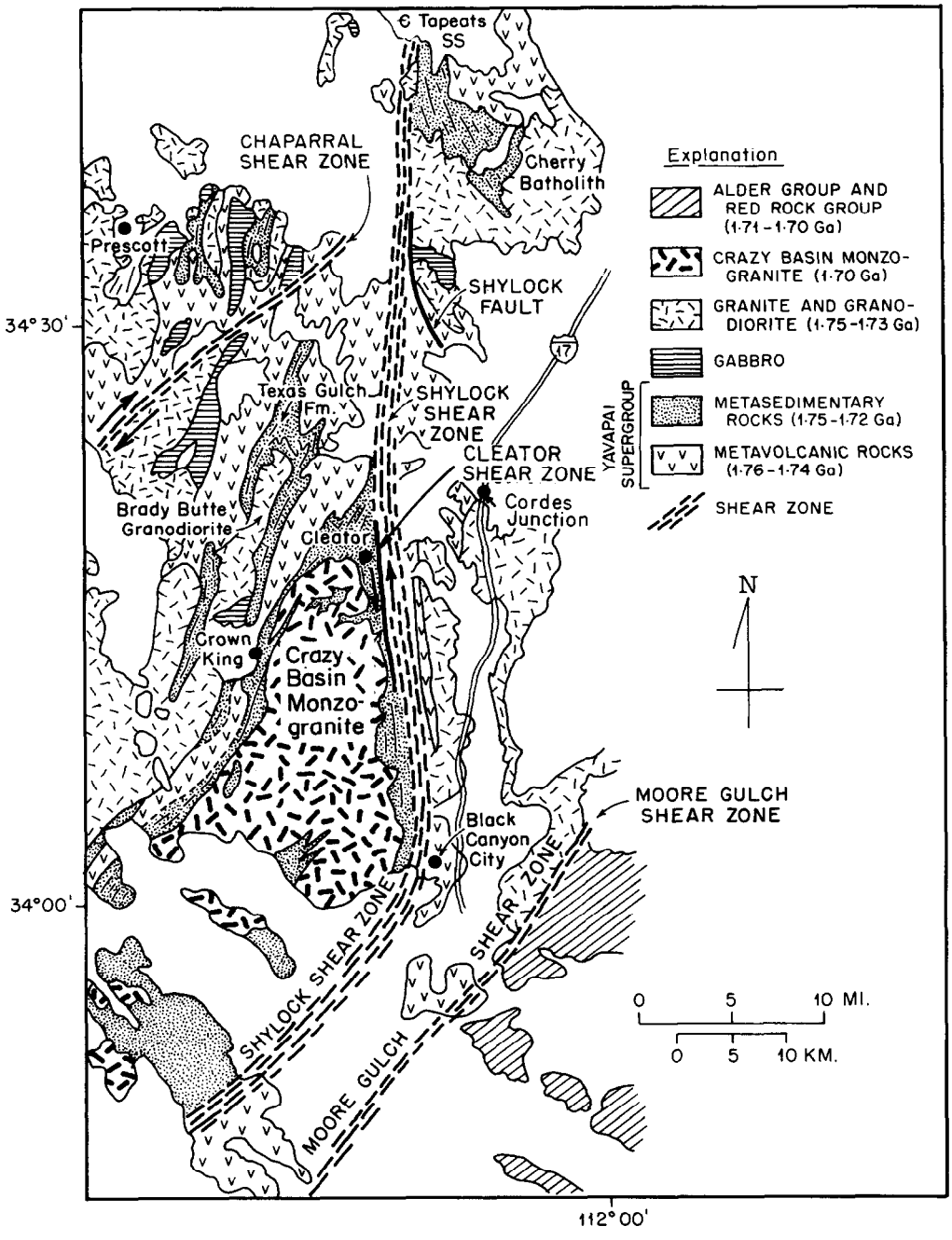

Fig. 2. Map of central Arizona showing the Crazy Basin Monzogranite and stratigraphic relationships in surrounding country rock. Big Bug block is bounded by the Chaparral and Shylock shear zones.

Geology of the Big Bug block

The Big Bug block (Fig. 2) contains volcanogenic rocks assigned to the Yavapai Supergroup (Anderson *et al.* 1971, Karlstrom 1989a). U–Pb zircon dates on volcanic rocks of the Yavapai Supergroup are about 1.76–1.74 Ga, with dates on the voluminous cross-cutting granodiorite plutons of *ca* 1.75–1.73 Ga (Karlstrom *et al.* 1987). The volcanic packages and the granodiorites are interpreted to have island arc affinities (Vance 1989, Anderson 1989, DeWitt 1989). In many areas, the volcanic rocks are uncomformably overlain by sequences of metamorphosed lithic sandstones, pelitic siltstones, and slates.

The Big Bug block records two or more major phases of deformation: (1) early recumbent folding, and (2) crustal shortening by upright folding (Karlstrom & Bowring 1991, Darrach *et al.* 1991, Bergh & Karlstrom 1992). All of the plutons in this block either pre-date or are synchronous with the crustal shortening. The earliest deformation produced a tectonic layering that strikes N–NW in areas where it has not been strongly reoriented by younger events. However, in most areas, this early fabric was folded by upright folds with a well-developed subvertical NE-striking foliation and steeply-plunging stretching lineation (Karlstrom 1989a). This NE-striking fabric is the dominant fabric in the Big Bug block.

The Shylock shear zone is a zone of well-developed subvertical foliation and lineation that bounds the Big Bug block on its east side (Figs. 2 and 3). Fabrics are

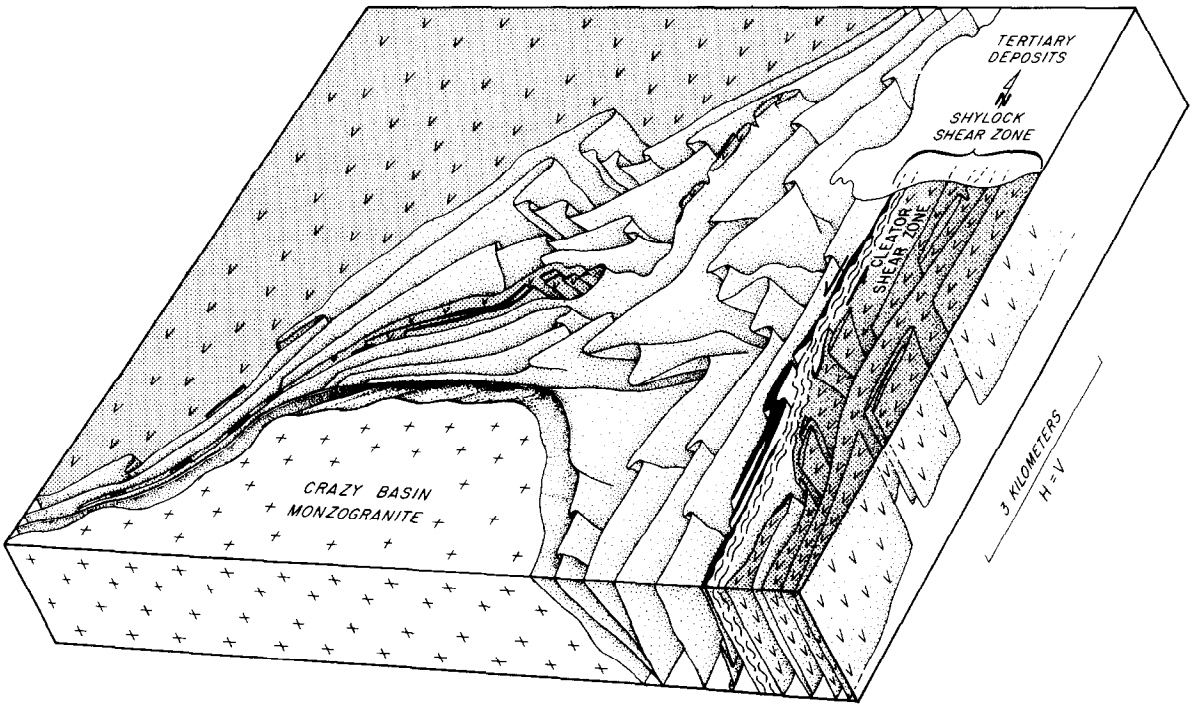

Fig. 3. Block diagram showing the geometry of folds around the north margin of the Crazy Basin Monzogranite. The repetition of volcanic rocks (v-pattern) across strike suggests a subhorizontal fold envelope for upright folds. Horizontal = vertical scale. V = metavolcanic rocks, dots = metasedimentary rocks, black = iron formation and chert, pluses = Crazy Basin Monzogranite.

contiguous from the Big Bug block into the Shylock shear zone. Although the shear zone shows some E-side-up dip-slip movements that are interpreted to be related to early thrusting, the main fabric of the zone involves second generation upright folds, N-striking subvertical foliation, and W-side-up movements (Darrach *et al.* 1991).

The late stage of progressive shortening in central Arizona was inhomogeneous and involved components of strike slip on conjugate shear zones. The Cleater shear zone is a discrete N-striking shear zone within the Shylock zone that shows sinistral strike-slip/W-side-up oblique movements. The NE-striking Chaparral shear zone shows dextral/E-side-up movements (Bergh & Karlstrom 1992) (Fig. 4). In this context, the sinistral slip on the Cleater zone is interpreted in terms of partitioning of oblique NW–SE shortening contemporaneous with emplacement of the Crazy Basin Monzogranite (Fig. 4), as discussed below. This interpretation of syntectonic emplacement follows Jerome (1956), Karlstrom & Argenbright (1985), Karlstrom & Conway (1986), Conway *et al.* (1987) and Anderson (1989), but conflicts with the post-tectonic interpretations of Jaager & Palache (1905), Anderson (1956), Blacet (1968, 1985), DeWitt (1976) and O'Hara (1980).

All rocks in the Big Bug block were metamorphosed to the greenschist or amphibolite facies. Previous workers have noted a general increase in metamorphic grade from north to south towards the Crazy Basin Monzogranite (Jaager & Palache 1905, O'Hara 1980, Blacet 1985). This has been interpreted as (1) a regional metamorphic gradient independent of the Crazy Basin pluton (O'Hara 1980), or (2) a contact metamorphic gradient superimposed on the regional isograds (Blacet 1966, 1985, DeWitt 1976). In contrast, we suggest that peak metamorphic porphyroblasts near the pluton grew during the regional deformation and metamorphism but reflect additional heat from crystallizing pluton (Williams & Karlstrom 1990). Their fabrics and spatial distribution document the synchroneity of regional deformation, peak metamorphism and plutonism.

Character of the Crazy Basin Monzogranite

The Crazy Basin Monzogranite is located in the southeastern part of the Big Bug block, adjacent to the Shylock shear zone (Fig. 2). The main mass of the Crazy Basin Monzogranite occupies an area of about 260 km^2, and it may extend in the shallow subsurface to the south, west and north (Burr 1991, Leighty *et al.* 1991) The intrusion is treated here as a single pluton although there are different units that probably represent distinct intrusive events. For example, in the northern part of the pluton there are two units: a main unit of medium-grained two-mica monzogranite and distinct megacrystic unit of two mica monzogranite (Blacet 1985) (Fig. 5). At least one area in the center of the pluton appears to be a roof pendant or screen of older granodiorite (DeWitt 1989) and the presence of many screens and xenoliths of country rock suggests numerous pulses of emplacement of concordant sheets of granite. The pluton also contains abundant cogenetic pegmatites, aplites and quartz or quartz-tourmaline veins.

Geochronologic investigations have been carried out on minerals from several areas of the Crazy Basin Monzogranite. U–Pb zircon data are quite discordant

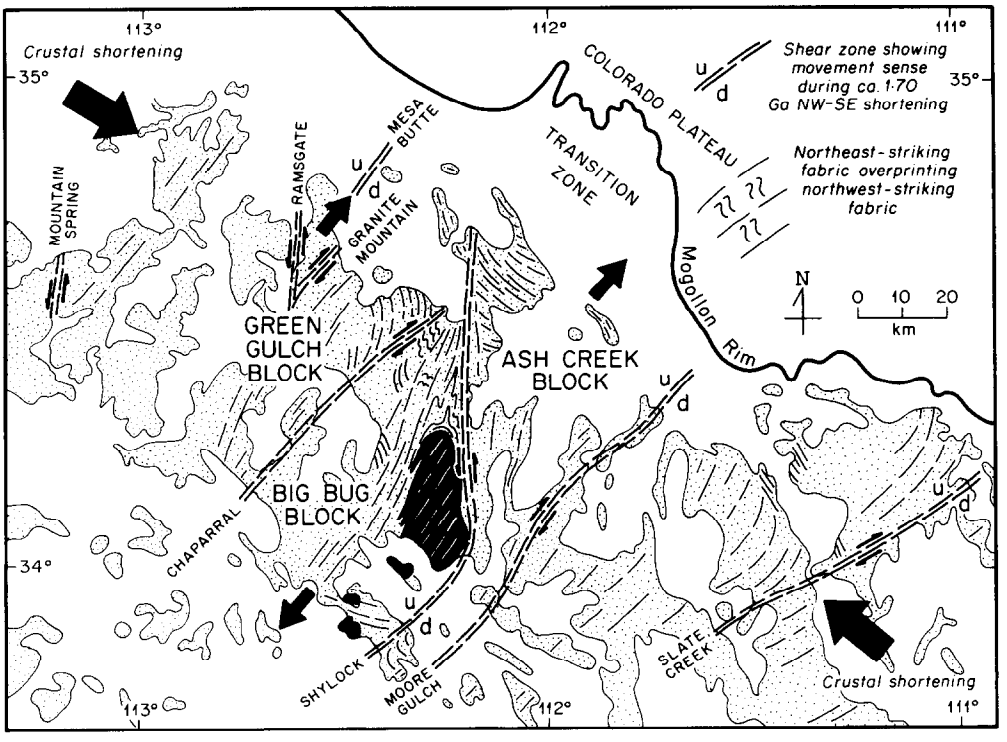

Fig. 4. Kinematic framework for NW–SE shortening (Bergh & Karlstrom 1992). The NE-striking foliation records NW–SE shortening at *ca* 1.70 Ga; shear zones are high strain zones; conjugate movements on shear zones in late stages of shortening accommodated further orogenic shortening by tectonic escape (movement of blocks shown by arrows). Black is Crazy Basin Monzogranite, light stipple represents other Proterozoic rocks, form lines represent 1.7 Ga and older Proterozoic fabrics.

but discordia lines point to ages close to 1.70 Ga. U–Pb sphene ages are about 1.695 Ga, which suggest relatively rapid cooling through 500 °C at this time (Bowring 1987 unpublished data). A conventional K–Ar date on muscovite from pegmatite is about 1.50 Ga (Shafiqullah *et al.* 1980), and $^{40}Ar/^{39}Ar$ plateau dates on muscovite from the northern margin of the pluton are 1.40–1.45 Ga (Hodges *et al.* 1994, Copeland personal communication). However, analysis of laser spot fusion $^{40}Ar/^{39}Ar$ data shows muscovites are zoned, with cores of >1.6 Ga and rims of <1.3 Ga and that the plateau and K–Ar dates represent the average gas age of slow-cooled muscovite grains with large diffusional gradients (Hodges *et al.* 1994). These data are consistent with a model involving rapid cooling to greenschist conditions followed by slow isobaric cooling in the middle crust (Bowring & Karlstrom 1990).

TIMING OF DEFORMATION AND PLUTONISM

Several lines of evidence suggest that the Crazy Basin Monzogranite crystallized in the late stages of NW–SE orogenic shortening. Pegmatite and aplite dike arrays around the pluton cross cut the regional shortening fabric but are themselves folded and foliated; their geometries suggest that emplacement was controlled by local extension compatible with regional strains. Parallel magmatic and solid state deformational fabrics within the pluton indicate syntectonic emplacement (Paterson *et al.* 1989). Likewise, foliation is deflected around the northern margin of the pluton (Fig. 6), forming a foliation triple point similar to those seen around other syntectonic plutons (Brun & Pons 1981). On a larger scale, the parallelism of the east margin of the pluton and the Shylock shear zone, with neither one cross-cutting the other, suggests their synchronous development. These lines of evidence are discussed below and summarized in Table 1.

Dikes, sills and vein systems

The northern contact of the Crazy Basin Monzogranite is a zone tens to hundreds of meters wide that was pervasively injected by dikes and sills of monzogranite, pegmatite, aplite and vein quartz. These injections decrease in abundance away from the pluton. Quartz veins, pegmatites, aplites and monzogranite dikes are mutually cross-cutting (Fig. 7a) and are interpreted to represent a continuum of melt and fluid interaction during pluton crystallization.

Aplite dikes are present in many areas but are most notable as several meter-thick dikes northwest and north of the pluton. One prominent dike swarm directly north of the pluton cross cuts the S_2 schistosity and both limbs of a large, nearly isoclinal antiform (Fig. 5). The dikes are weakly folded and contain the S_2 schistosity, but they also contain xenocrysts of syn-S_2 biotites (Fig. 8a). We infer that dike intrusion occurred near the end of the phase of crustal shortening. U–Pb zircon data from the dike show strong discordance, but points fall on the same discordia line as the Crazy Basin pluton

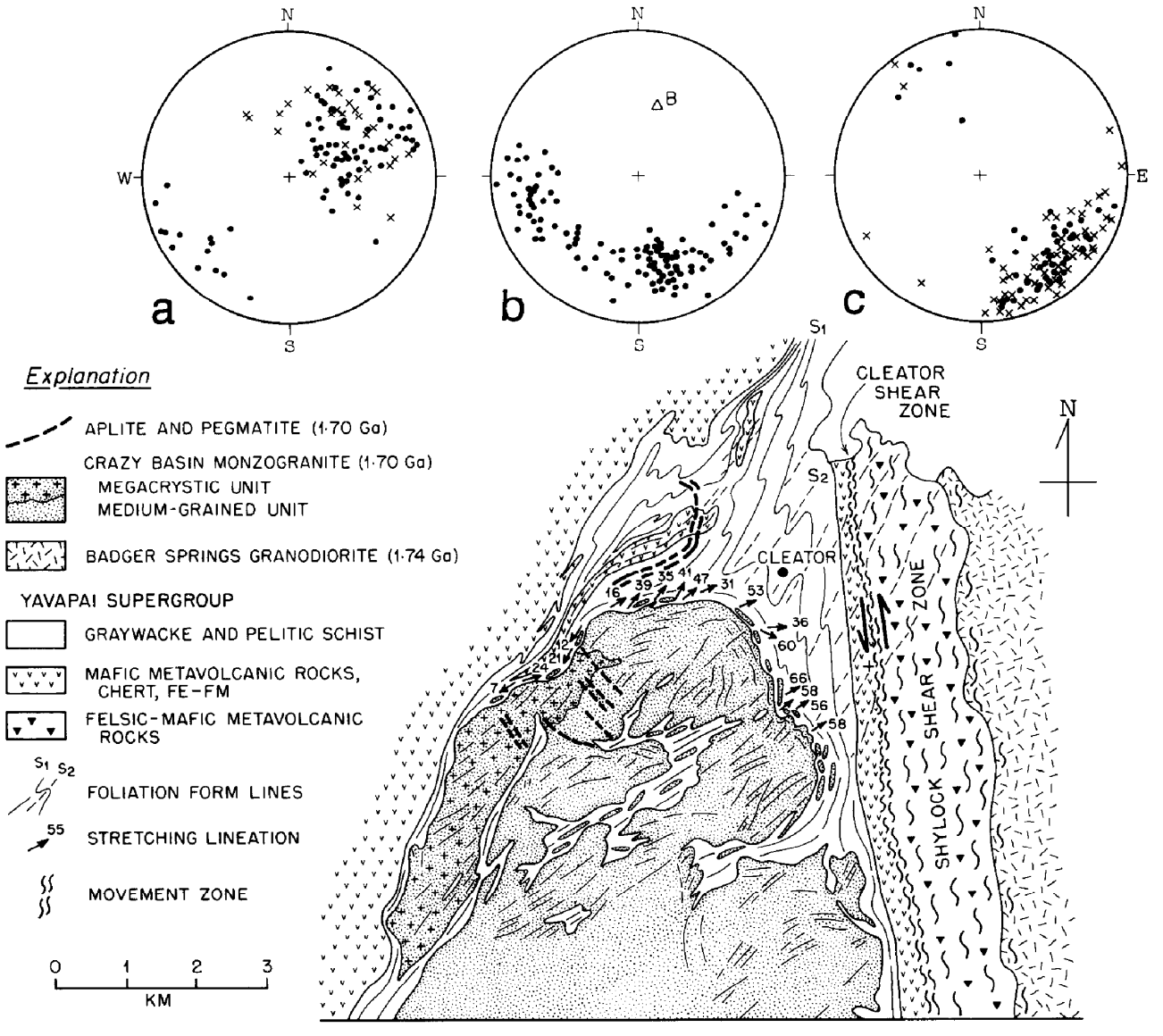

Fig. 5. Fabric elements in the vicinity of the northern Crazy Basin Monzogranite. Lower hemisphere equal area projections: (a) Lineations (dots = mineral elongation lineations; crosses= necks of boudins); (b) Poles to foliation in the pluton margin define a girdle indicating the northward plunge (B) of the northern pluton contact; (c) Poles to foliation in the pluton (dots= solid state foliations; crosses = magmatic foliation in the megacrystic unit). Note that the megacrystic unit occupies a discrete body on the west side of the pluton.

suggesting that they are coeval at approximately 1.70 Ga (Bowring personal communication).

Near the northeast and east sides of the pluton, granites, as well as pegmatites and quartz–tourmaline veins fill dike and vein arrays (Fig. 6). Dikes and veins have geometries compatible with left-lateral strike-slip shearing along the margin of the pluton, and are thus compatible with movements in the Cleater shear zone. Several give a right lateral sense of shear, but these are within the triangle zone north of the pluton (discussed later). The dike and vein arrays provide convincing evidence for the presence of melt and fluids during deformation. Rotated quartz and granite veins cross cut by straight veins suggest emplacement during progressive simple shear. The consistent sinistral sense of movement around the pluton is difficult to understand in terms of emplacement-related strains, and is more readily understood in terms of distributed shear deformation during and after granite crystallization.

An array of late-stage pegmatite dikes cross cut the megacrystic and main units in the northwest part of the pluton. These dikes strike NW and dip steeply NE (Fig. 5). Because they are tabular, undeformed, and cross cut magmatic and solid state fabrics and the pluton margins, their orientation reflects the incremental strain field during their emplacement. They suggest NW–SE shortening and subhorizontal NE extension, compatible with the regional shortening deformation. Some of the pegmatites have a more easterly strike; these display deformed margins (Fig. 7b) and are inferred to have rotated during the sinistral shearing that affected the northwest side of the pluton during and after crystallization of the megacrystic unit and pegmatites.

Granite sills and dikes in the contact zone are com-

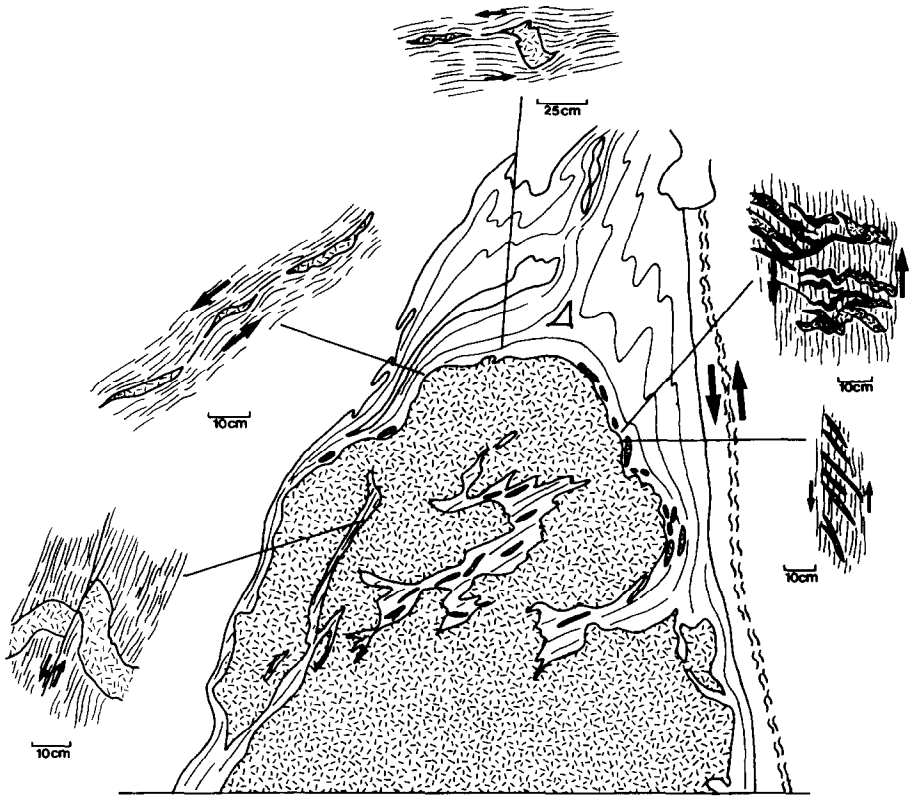

Fig. 6. Geometry of dikes, sills and vein arrays around the northern margin of the Crazy Basin Monzogranite. The foliation triple point of the north side of the pluton is shown as a triangle.

positionally similar to the main unit of the Crazy Basin Monzogranite. They are subparallel to schistosity, foliated, and boudinaged. Boudin necks are subparallel to the local stretching direction defined by elongate minerals in the country rock and boudinaged tourmaline crystals in quartz veins (Fig. 5), suggesting a component of chocolate tablet boudinage and local rotation of boundins towards the NE-plunging stretching direction. This stretching direction is subparallel to that of the Cleater shear zone (Darrach *et al.* 1991) suggesting a kinematic link between pluton emplacement and sinistral/W-side-up oblique movements in the Cleator shear zone.

Parallel magmatic and solid state fabrics

Another indication that melt participated in deformation is magmatic alignment of megacrysts. Magmas with less than 50–70% crystals (critical melt fraction, van der Molen & Paterson 1969) cannot sustain appreciable shear stress, and megacryst alignments are interpreted to reflect quasi-viscous flow. As magma passes through its critical melt fraction, it develops an increasingly strong grain network (Miller *et al.* 1990). If this occurs during regional deformation, magmatic fabrics can be parallel to, and transitional into, solid state deformation fabrics, with both kinematically related to regional deformation (Paterson *et al.* 1989).

The megacrystic unit of the Crazy Basin Monzogranite contains a steeply NW-dipping foliation defined by euhedral K-feldspar and mica crystals (Fig. 7c). Most feldspars are not dynamically recrystallized, indicating that they were aligned by flow of magma. Locally, megacrysts define a magmatic-state *S–C* fabric (Blumenfeld & Bouchez 1988) indicating sinistral shear, compatible with the pattern of regional deformation (Fig. 7c). In some areas, megacrysts are rimmed by myrmekite and record subsequent solid state dynamic recrystallization (Simpson & Winch 1986) (Fig. 8c), which suggests deformation at temperatures in excess of 500 °C (Tullis 1983, Simpson 1985, Gapais 1989, Simpson & DePoar 1991). This is compatible with solid state deformation during and after crystallization.

The NE strike of foliation defined by aligned feldspar and mica phenocrysts is compatible with flow of magma parallel to the NE-trending pluton margin (Blacet 1985). However, in some areas this megacrystic fabric is at a high angle to a local pluton or dike margin (Fig. 7d). This is difficult to reconcile with magmatic flow because pluton and dike margins generally influence flow. Further, the megacrystic fabric in these areas is continuous with deformation fabrics in the adjacent country rocks. We infer that there was little difference in effective viscosity across the contact and that megacrysts were aligned perpendicular to regional contraction during final cooling.

Xenoliths

Xenoliths and screens of country rock are abundant in most areas of the Crazy Basin Monzogranite (Fig. 5). In

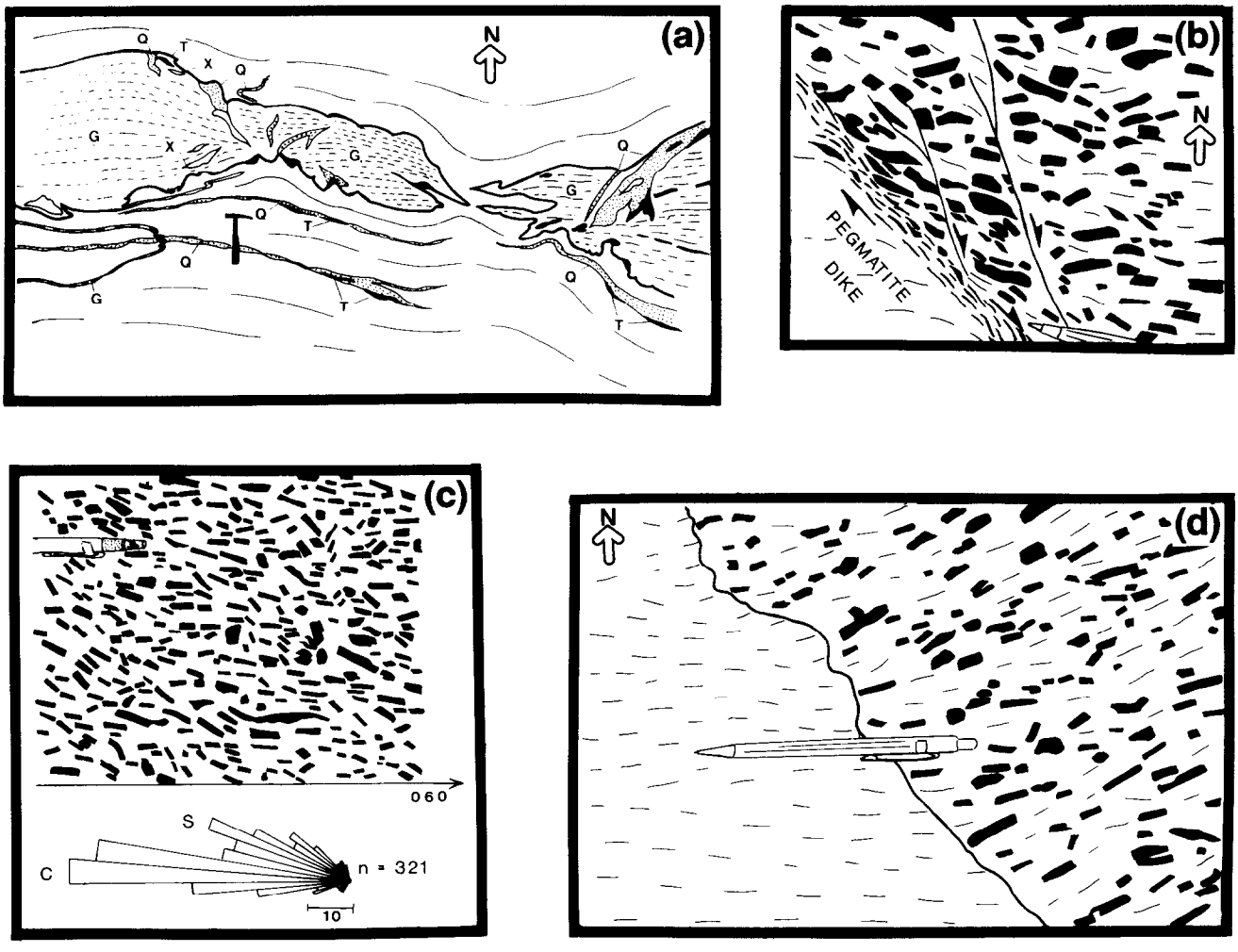

Fig. 7. Field sketches: (a) Sketch of mutually cross-cutting injections of granite = G and quartz = Q—tourmaline = T veins. Note that small granite dike left of hammer cross-cuts quartz-tourmaline vein. X = xenoliths; form lines show foliation in country rock schist (long lines) and granite sill (short lines). (b) NW-striking pegmatite cross-cuts fabric; Magmatic fabric is deflected at the dike margin due to antithetic slip as pegmatite rotated in response to sinistral shear. Note zone of reduced grain size at contact indicating solid-state deformation. Exposed portion of pen is about 2 cm long. (c) Megacrysts define a magmatic-state *S–C* fabric; Histogram shows orientations of 321 megacrysts relative to a reference plane (strike 060) that is interpreted to represent the plane of magmatic flow. Exposed portion of pencil 6 cm long. (d) Magmatic foliation of megacrysts at high angle to contact between fine-grained (left) and megacrystic units; foliation is continuous across the contact. Pencil is 15 cm long.

the southern and eastern areas, the pluton is essentially an injection migmatite, with as much as 50% of outcrops composed of metasedimentary country rock (Kortimier 1984, Burr 1992). In these areas, the pluton consists of a swarm of tabular sheets that strike NE, generally parallel to the foliation in the country rocks. Xenoliths and screens contain well developed S_1 and S_2 foliations, indicating that the pluton post-dated much of the regional shortening strain. Granites in these areas also contain the S_2 cleavage and have themselves undergone some of the shortening, supporting the syn-shortening time emplacement.

In the northeast margin of the pluton, the medium-grained unit of the granite shows both a margin-parallel fabric (see below) and a NE-striking fabric. Long axes of xenoliths in this area have a northeasterly strike, parallel to the regional foliation (Fig. 5). These xenoliths were probably aligned in the presence of melt during regional contraction.

Marginal foliation and foliation triple point

Besides the dominant NE-striking regional foliation, a variably-developed foliation also parallels the northern margin of the pluton in both granite and country rock. The marginal fabric is the dominant fabric within 500 m both sides of the pluton margin. It is characterized by aligned mica and dynamically recrystallized feldspar and quartz aggregates and is axial planar to folded granite dikes. The marginal fabric becomes less pronounced inward toward the center of the pluton; the inner parts of the pluton are generally dominated by the NE-striking regional fabric. Approximately 500 m in from the margin, regional and marginal fabrics coexist, but both fabrics are quite indistinct and the nature of their interaction (overprinting?) is unknown. We interpret the marginal fabric to have been produced during emplacement of the pluton, and to be primarily controlled by local strains rather than regional deformation.

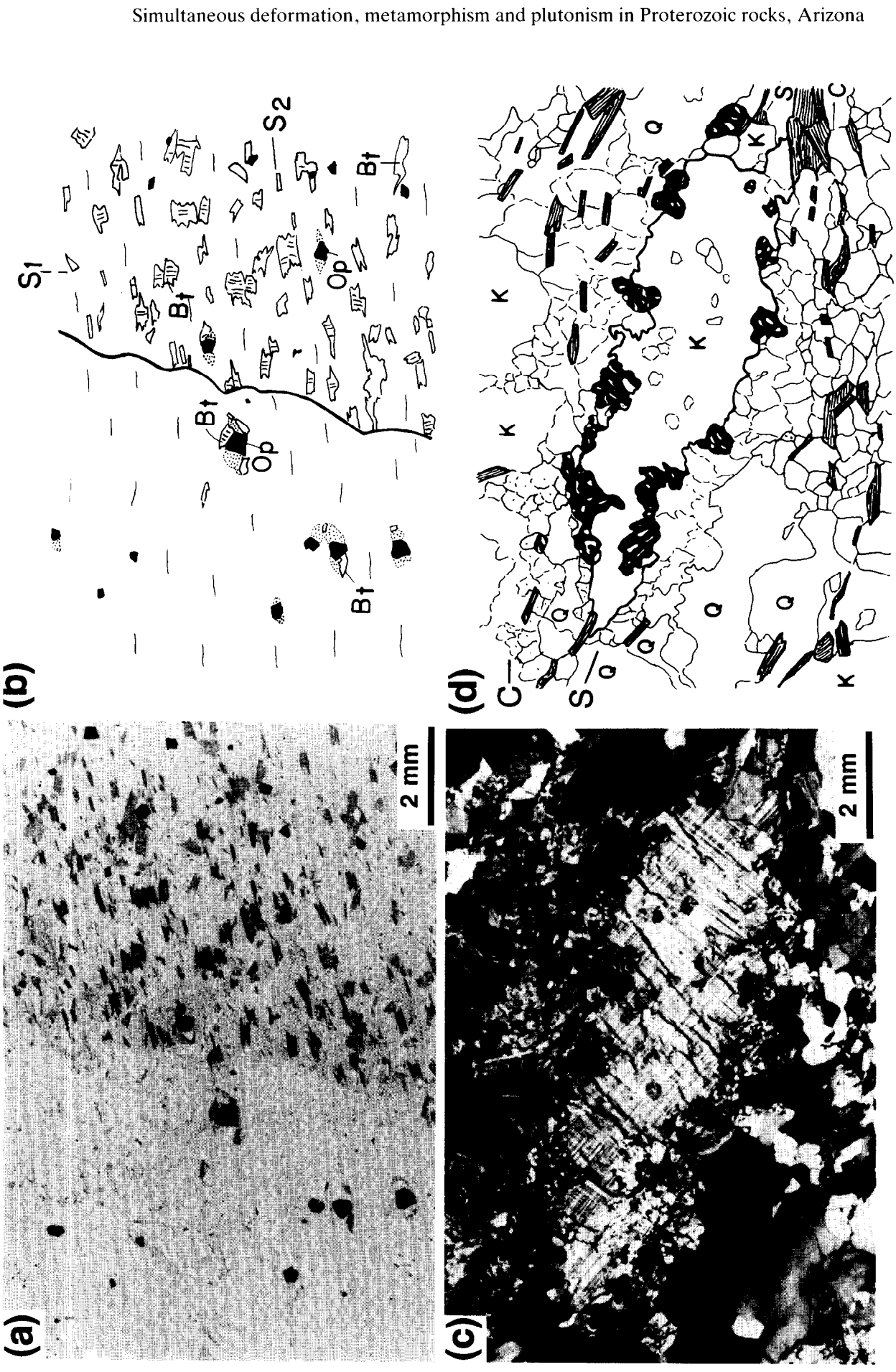

Fig. 8. Photomicrograph (a) and sketch (b) of the weakly-folded contact between aplite (left) and country rock. S_2 fabric is developed in both dike and country rock. However the dike contains xenocrysts of the aligned syn-S_2 biotite porphyroblasts with inclusion trails as well as opaque grains with S_2-related pressure shadows. Since xenocrystic biotites are identical to those of country rock, they must have existed as part of the S_2 cleavage before dike intrusion. S_1-related inclusion trails in biotites are straight to very weakly crenulated and subparallel in all porphyroblasts, indicating little rotation of biotites during shortening. Photomicrograph (c) and sketch (d) of solid state recrystallization of K-feldspar megacryst = K. Myrmekite (black with white blebs) occurs within a zone of dynamically recrystallized K-feldspar on the high strain faces of the porphyroclast. Biotite (lines) defines both *S*- and *C*-planes; this *S*–*C* fabric may have

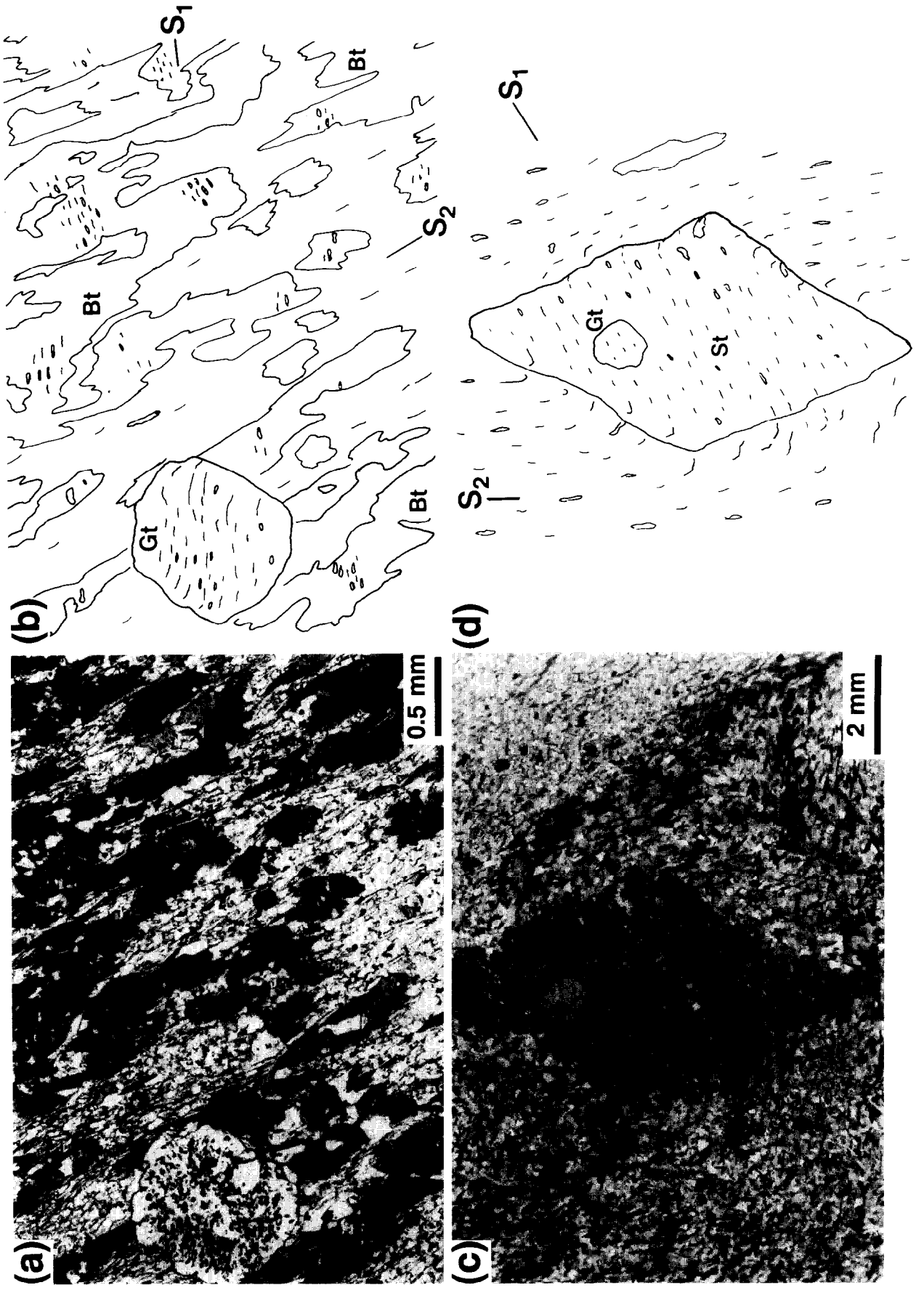

Fig. 14. Photomicrograph (a) and sketch (b) of garnet–biotite–chlorite–muscovite–plagioclase–quartz schist from the Crazy Basin area. This sample was used for *P–T–t* analysis (Fig. 12). The weakly-crenulated inclusion trails are parallel in all garnet and biotite porphyroblasts throughout the thin section indicating non-rotational porphyroblast growth. (c) Photomicrograph and sketch (d) of early staurolite crystal overgrowing a single asymmetric S_2 crenulation. Note that inclusion trails are continuous from included garnet to staurolite suggesting little fabric development between staurolitic and garnet development.

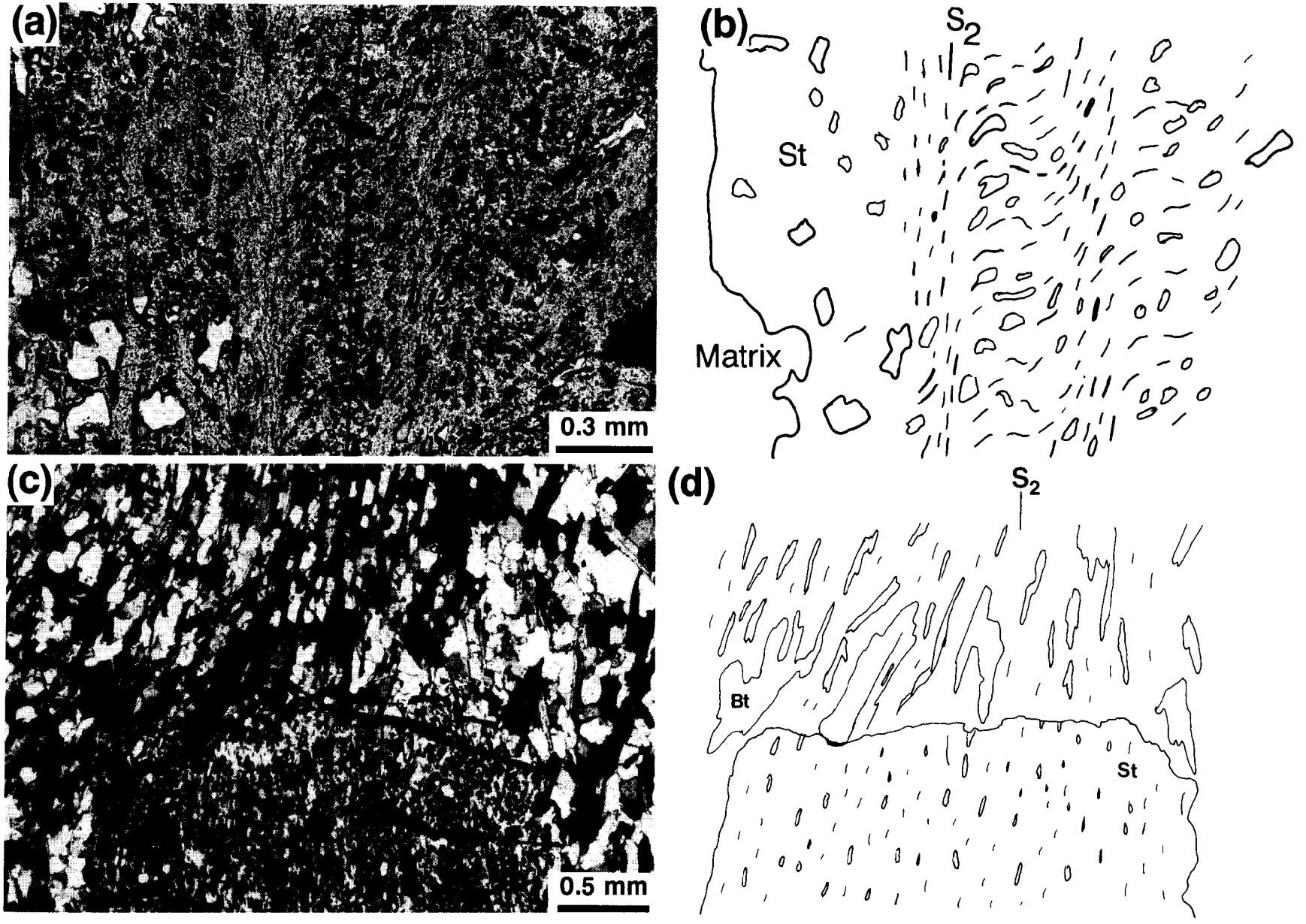

Fig. 15. Photomicrograph (a) and sketch (b) of staurolite porphyroblast overgrowing an S_2 differentiated crenulation cleavage. The inclusions consist of quartz, plagioclase, biotite, muscovite and ilmenite. Note that inclusions in inclusion-rich domains are generally aligned perpendicular to the domain boundaries, and in the clearest examples, curve continuously, while grain size diminishes, into the inclusion-poor domains. Inclusion-poor domains represent microlithons of relatively intense cleavage formation where phyllosilicate/quartz ratios were high due to progressive dissolution of quartz. Inclusion-rich domains represent low-strain microlithons near the hinges of crenulations where phyllosilicate/quartz ratios were lower, probably more typical of the S_1-dominated fabric before the onset of shortening. (c) Photomicrograph and sketch (d) of staurolite porphyroblast overgrowing penetrative S_2 cleavage continuous with matrix fabric, with coarsening of S_2-defining minerals and continued shortening across S_2 after staurolite growth.

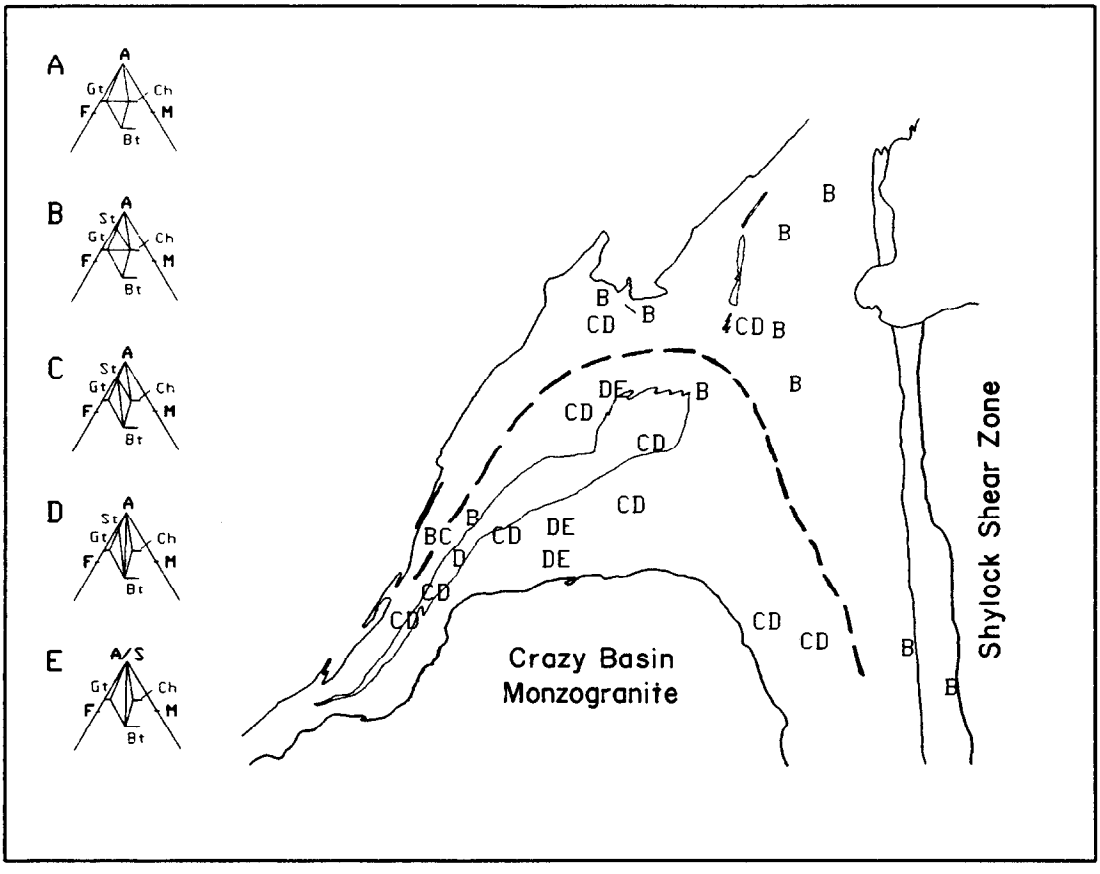

Fig. 9. Distribution of metamorphic mineral assemblages and AFM topologies near the northern margin of the Crazy Basin Monzogranite. Heavy dashed line shows the approximate position of the first occurrence of a staurolite+biotite or andalusite+biotite tie line (see text for discussion).

Immediately northeast of the pluton, fabrics in the country rock form a 'triple point' (Fig. 6). This resembles foliation triple points associated with many plutons (Brun & Pons 1981) and often attributed to combined effects of diapiric emplacement and regional deformation. Such a model may also apply in the Crazy Basin area. We do not interpret the triple point as a strain shadow around a pretectonic pluton because there is evidence for participation of melts, emplaced as dike arrays, within the triple point. These vein arrays indicate dextral rather than the regional sinistral movements (Fig. 6), but complex movement histories are a feature also attributed to syntectonic triple points (Brun & Pons 1981).

Finally, it is important to note that the country rock near the pluton is characterized by a zone 100–300 m wide where pelitic rocks are friable, and richer in sericite and muscovite than pelitic rocks far from the pluton. Porphyroblast-bearing layers can be traced across this zone but they are less common here than farther from the pluton. Mineral assemblages suggest that the zone is not a product of prograde metamorphism. Instead, it may be a zone of metasomatism related to passage of fluids during or after crystallization of the pluton. Fabric in this zone is continuous with fabrics in the pluton and the country rock away from the pluton so, whatever the time of metasomatism, we infer that the fabric patterns were formed during the interaction of regional deformation and pluton emplacement.

TIMING OF PLUTONISM AND METAMORPHISM

The distribution of mineral assemblages indicates that metamorphic grade increases towards the pluton. Quantitative thermobarometry confirms that peak metamorphic temperatures were progressively higher towards the pluton at relatively constant pressure. Metamorphic data are well explained by thermal models in which the pluton is a shortlived heat source that locally elevated peak regional metamorphic temperatures.

Distribution of assemblages and isograds

Metamorphic mineral assemblages are systematically distributed with respect to the margin of the Crazy Basin Monzogranite (Fig. 9). Pelitic rocks farthest from the pluton (some 4–6 km north) contain quartz, muscovite, chlorite, albite, +/− biotite, and Mn-rich garnet. Nearer to the pluton, pelitic rocks contain various combinations of quartz, muscovite, biotite, chlorite, garnet, plagioclase, staurolite, and andalusite; mafic rocks contain hornblende, plagioclase, biotite, +/− garnet. At the pluton margin (DeWitt 1976) and in pelitic xenoliths and

screens within the pluton, sillimanite occurs with muscovite, quartz, garnet, and biotite.

Although the distribution of assemblages shows higher grade metamorphism near the Crazy Basin Monzogranite, the geometry of the isograds is complicated and obscured by compositional variation within the supracrustal sequence. In pelitic rocks, variations in Fe/(Fe+Mg) is indicated by AFM phase relationships (Fig. 9), and the Mn-content of garnet varies widely (mole percent spessartine ranges from zero to more than 0.30). The various lithologies are interlayered at a fine scale such that several mineral assemblages may be present even within a single hand specimen. Consequently, many assemblages appear to be univariant or even invariant, and it is difficult to identify the 'peak' equilibrium assemblages in many samples.

Five-AFM-phase assemblages with garnet, biotite, chlorite, staurolite, and andalusite are relatively common in the Crazy Basin area (Fig. 9). In many of these rocks garnet is believed to be stabilized by the 'extra' manganese (Pattison & Tracy 1991, Symmes & Ferry 1992). Foliated chlorite is present in nearly all assemblages, but textures suggest it is commonly a retrograde (i.e. disequilibrium) phase. Relationships between staurolite and andalusite are complicated, and evidence for the nature and timing of reactions is rare. At least some of these rocks appear to contain two finely interlayered assemblages, (1) staurolite–biotite +/− garnet, and (2) andalusite–chlorite +/− biotite, representing two bulk compositions.

Except for the polymorphic transition of andalusite to sillimanite which occurs near the pluton margin, it is difficult to map metamorphic isograds in the Crazy Basin area. Staurolite was apparently produced by at least three reactions,

$$\text{garnet} + \text{chlorite} + \text{andalusite} = \text{staurolite} + \text{quartz} + H_2O \quad (1)$$

$$\text{garnet} + \text{chlorite} = \text{staurolite} + \text{biotite} + \text{quartz} + H_2O \quad (2)$$

$$\text{chlorite} + \text{muscovite} = \text{staurolite} + \text{biotite} + \text{quartz} + H_2O \quad (3)$$

and andalusite may also have been produced by at least three reactions:

$$\text{pyrophyllite} = \text{andalusite} + \text{quartz} + H_2O \quad (4)$$

$$\text{staurolite} + \text{chlorite} = \text{andalusite} + \text{biotite} + H_2O \quad (5)$$

$$\text{staurolite} = \text{andalusite} + \text{garnet} + \text{biotite}. \quad (6)$$

These reactions may have occurred at significantly different times in the P–T history due to the variations in the local bulk composition. In Al-rich bulk compositions, andalusite was produced by reaction (4) in some of the lowest-grade rocks, well below the temperature of staurolite-producing reactions. In Mg-richer compositions, staurolite and andalusite may have been produced at nearly the same temperature by reactions (3) and (5), respectively. Finally, in Fe-rich assemblages, andalusite (and locally sillimanite) was produced by reaction (6), after staurolite, only in the highest grade rocks.

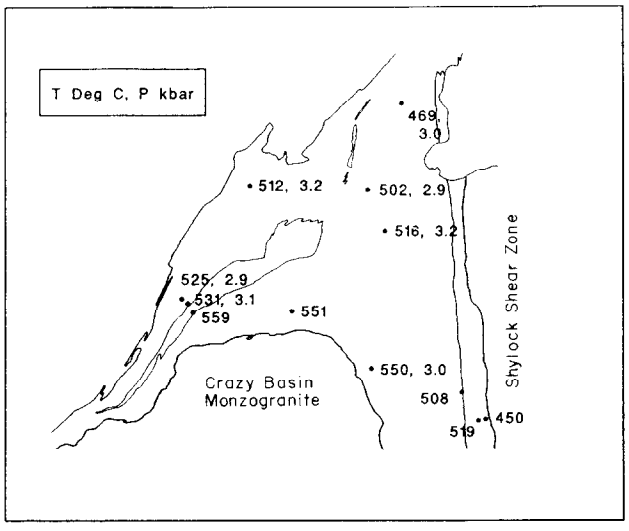

Fig. 10. Calculated temperatures and pressures for selected samples in the Crazy Basin area. Temperatures are based on the garnet–biotite thermometer as calibrated by Ferry & Spear (1978) and modified to incorporate the effects of non-ideal mixing of Mn in garnet (Williams & Grambling 1990). Pressures are based on garnet–biotite–plagioclase–muscovite barometry (Ghent & Stout 1981, Hodges & Crowley 1985, Hoisch 1990). Absolute errors are on the order of 50°C and 1 kb, but relative errors are significantly smaller (Hodges & Crowley 1985).

In many metamorphic terranes, reaction (2) can be a useful isograd for regional metamorphic mapping, but in the Crazy Basin area this reaction is at least divariant due to the widely varying X_{sps}. Further, as noted above, it is extremely difficult to distinguish peak from retrograde chlorite because both types tend to display similar deformational fabrics. With these complications in mind, the approximate position of the first staurolite–biotite tie line (reaction 2) is shown in Fig. 9.

Metamorphic conditions certainly increase from north to south in the Crazy Basin area, and similar gradients are observed at the southern and eastern margins of the pluton (Burr 1991). However, because of compositional complexity, phase relations cannot unequivocally distinguish between models in which the gradient reflects additional heat from crystallizing pluton (Blacet 1968) from models in which there is regional metamorphic gradient independent of the pluton (O'Hara 1980).

Quantitative thermometry and barometry

Metamorphic temperatures and pressures calculated for 12 samples from the Crazy Basin area support a model involving pluton enhanced metamorphism (Fig. 10). Data from three separate areas, all more than 10 km from the Crazy Basin pluton, suggest that peak regional metamorphic temperatures were as low as 400 °C (Burr 1991, Williams 1991). In the Crazy Basin area, temperatures increase from 460°C away from the pluton to

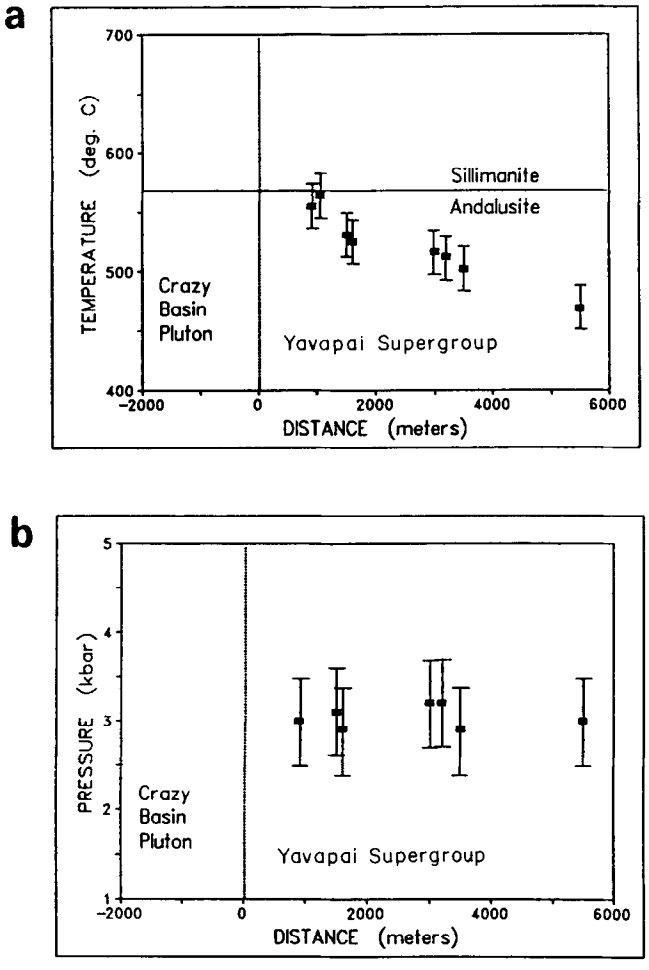

Fig. 11. Plots of calculated temperature (a) and pressure (b) vs distance from Crazy Basin Monzogranite. Samples from Fig. 10 were projected to a roughly N-trending traverse away from the pluton. Error bars are ±50°C and 1 kb. Sillimanite/andalusite isotherm shown in (a) is for 3 kb.

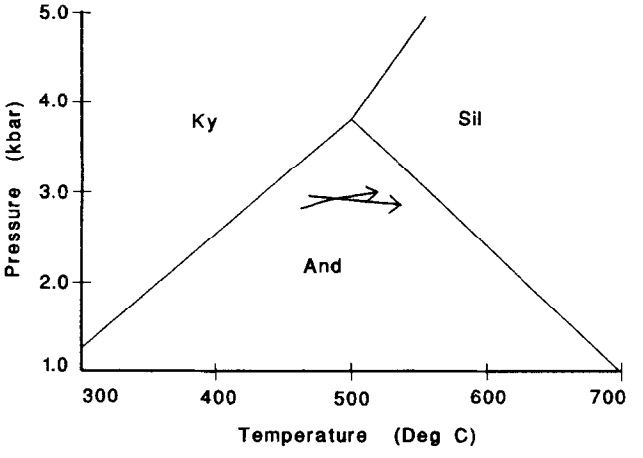

Fig. 12. *P–T–t* paths for two samples from the central Crazy Basin area (longer arrow corresponds to sample 525, 2.9 of Fig. 10; shorter arrow to sample 5, 6, 3.2). Both samples contain the assemblage garnet–biotite–chlorite–plagioclase–quartz–muscovite–ilmenite. *P–T* paths were calculated using the Gibbs method (Spear *et al.* 1982) on zoned garnets with plagioclase and biotite inclusions (Williams *et al.* 1994).

approximately 630°C near the pluton (Fig. 11a). Pressures are essentially constant at 3 kb, varying by only 0.3 kb (Fig. 11b), well within the estimated error of the geobarometer. The calculated temperatures and pressures are compatible with the phase relationships discussed above. Garnet and biotite are predicted to occur even in the lowest temperature samples, and sillimanite is expected in only the highest temperature samples immediately adjacent to the Crazy Basin pluton.

P–T–t paths have been calculated for two samples from the Crazy Basin area (Fig. 12) using the Gibbs method (Spear *et al.* 1982, Spear & Peacock 1989) and by direct calculation of temperature and pressure from host + inclusion assemblages. Both samples contain plagioclase and biotite inclusions near the cores of garnet porphyroblasts and one sample has several plagioclase inclusions between the core and rim. Matrix muscovite compositions were used for the direct pressure calculations as no muscovite inclusions were present. The results suggest isobaric heating; temperatures increased from approximately 450°C–550°C with little or no change in pressure.

Thermal history of the Crazy Basin area

Although fluids must have played a role in transporting heat from the crystallizing Crazy Basin Monzogranite, the variation in peak temperatures is consistent with a simple model involving conductive cooling of the pluton during regional metamorphism. Figure 13(a) shows the two-dimensional distribution of isotherms at six times in the cooling history. The isotherms were constructed assuming that the Crazy Basin Monzogranite is a roughly tabular intrusion, 4 km thick, emplaced near its solidus at approximately 700°C. The results suggest that, if the units of the Crazy Basin pluton are roughly coeval as supported by the geochronology, then the thermal effects of the emplacement and cooling are largely dissipated after approximately 1 Ma. Thus, the growth of peak metamorphic porphyroblasts near the pluton was rapid relative to typical regional deformation/metamorphic events. This is compatible with the interlayering of assemblages at hand sample scale which suggests limited mass transfer during a brief event.

Figure 13(b) shows the maximum temperature (T_{max}) attained at any point along the traverse away from the crystallizing and cooling pluton. Points farther from the pluton along the T_{max} line reflect later times in the cooling history compared to points near the pluton. Garnet–biotite temperatures from Fig. 11 are consistent with the conductive cooling model.

Thus, metamorphic data indicate that the Crazy Basin Monzogranite represents a short-lived thermal anomaly that was introduced into rocks undergoing regional greenschist facies metamorphism (400–450°C, 3 kb). All microstructures and phase relationships display characteristics typical of regional ('dynamothermal') metamorphism (see below). In order to distinguish it from anorogenic contact metamorphism, we refer to this metamorphic history as pluton-enhanced high

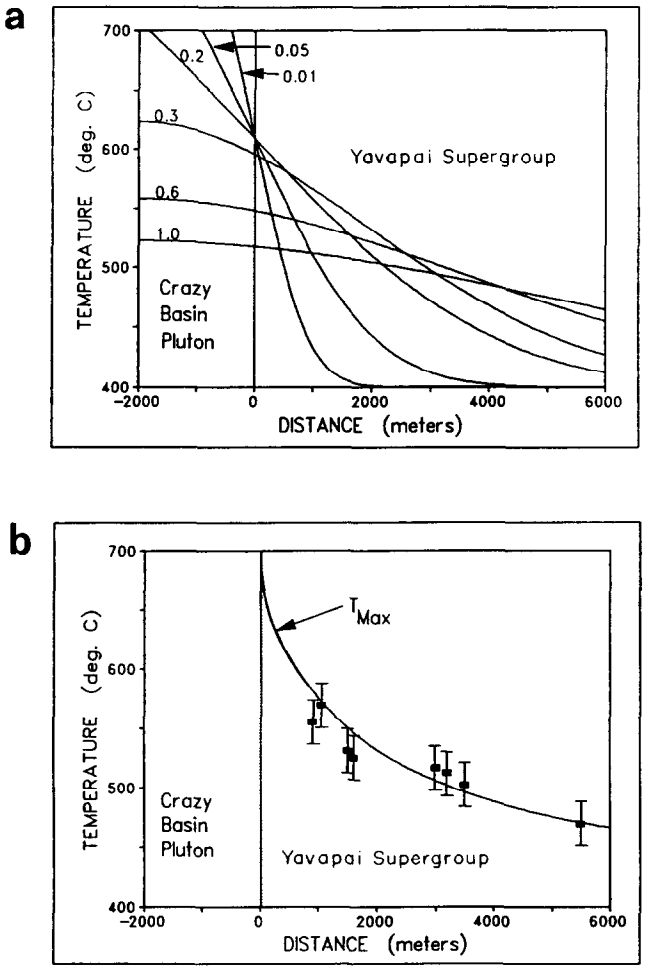

Fig. 13. Generalized conductive cooling model for the Crazy Basin Monzogranite. The pluton is assumed to have been emplaced at 700°C into rocks undergoing regional metamorphism at 400°C, 3 kb. Based on equations in Turcotte & Schubert (1982, p. 172) and Philpotts (1990). (a) Isotherms at fixed times in the cooling history. Isotherms at 0.01, 0.05 and 0.2 Ma represent the thermal effects associated with crystallization of the pluton. Isotherms at 0.3, 0.6 and 1.0 Ma reflect cooling of the completely solidified pluton. (b) Line represents the predicted maximum temperature (T_{max}) at any fixed distance from the pluton. Calculated temperatures from Fig. 11(a) (boxes with error bars) show close correspondence with the model.

temperature-low pressure regional metamorphism, similar to 'regional aureole' metamorphism of den Tex (1963). This general style of low P, high T metamorphism (Lux *et al.* 1986) may be characteristic of Proterozoic rocks across Arizona (Williams 1991) and other arc and back-arc settings (Barton & Hanson 1989).

TIMING OF METAMORPHISM AND DEFORMATION

Regional shortening was accommodated by the development of upright folds and the production of a steeply-dipping, N- to NE-striking S_2 schistosity. Inclusion relationships in porphyroblasts preserve microfolds of an early schistosity (S_1) and preserve various stages in the progressive development of the new schistosity (S_2), indicating that porphyroblasts grew during the development of S_2.

Garnet and biotite porphyroblasts in the Big Bug block contain simple straight or sigmoidal inclusion trails. The individual inclusions, typically quartz, albite or plagioclase with rarer biotite and tourmaline, are aligned and define an early shape preferred orientation. The straight trails and the axial planes of the sigmoidal trails are parallel from porphyroblast to porphyroblast within a thin section or even within a small outcrop (Fig. 14a). This parallelism strongly suggests that the curved trails did not develop from syntectonic rolling of porphyroblasts, but instead represent embryonic F_2 fold noses (Williams 1994). In most samples continued shortening has obscured most evidence in the matrix for the early F_2 crenulations.

Staurolite and andalusite in the Crazy Basin area preserve several inclusion morphologies, generally representing more advanced stages in the development of the S_2 cleavage than that observed in garnet and biotite. Some staurolite porphyroblasts overgrew single asymmetric F_2 crenulations (Fig. 14c), similar to those in garnet and biotite. However, the most common and distinctive inclusion morphology consists of alternating bands of inclusion rich and inclusion poor domains in a single staurolite or andalusite porphyroblast (Fig. 15a). This inclusion geometry apparently formed when staurolite or andalusite porphyroblasts overgrew a differentiated crenulation cleavage, stage 4 of Bell & Rubenach (1983). Where garnet coexists in a single thin section or hand specimen with staurolite or andalusite, the axial traces of included crenulations in garnet are generally parallel to the crenulation cleavage in staurolite or andalusite and also to rare tight fold noses in the matrix. This suggests that the included crenulation cleavage is a transitional stage in the evolution from the open folds preserved in garnet and biotite to the penetrative fabric preserved in the matrix, an interpretation that differs from Bell & Johnson (1989) who suggests that porphyroblasts only grow during early stages of crenulation cleavage development (Williams 1994).

A third inclusion geometry observed in staurolite and andalusite consists of straight or gently warped internal foliation that can be traced continuously into the predominant matrix foliation (Fig. 15c). In some crystals, the included foliation is parallel to the matrix foliation and in other crystals, they diverge by up to 30°. Where they are non-parallel, the included foliation typically curves into parallelism with the matrix fabric within the outermost several millimeters of the porphyroblast. Inclusion phases are generally finer in size than equivalent phases in the matrix. Porphyroblasts with this microstructure are interpreted to have overgrown a nearly completely formed S_2 schistosity, that was coarsened and locally reoriented after porphyroblast growth.

Chlorite, a ubiquitous mineral in the Crazy Basin area, can be both a prograde and retrograde phase. Many samples show evidence for late-stage (retrograde) chlorite growth: chlorite occurs as beards and rims on garnet, staurolite, and andalusite porphyroblasts and some biotite crystals are partially altered to chlorite. In other samples, chlorite is consistent with local AFM

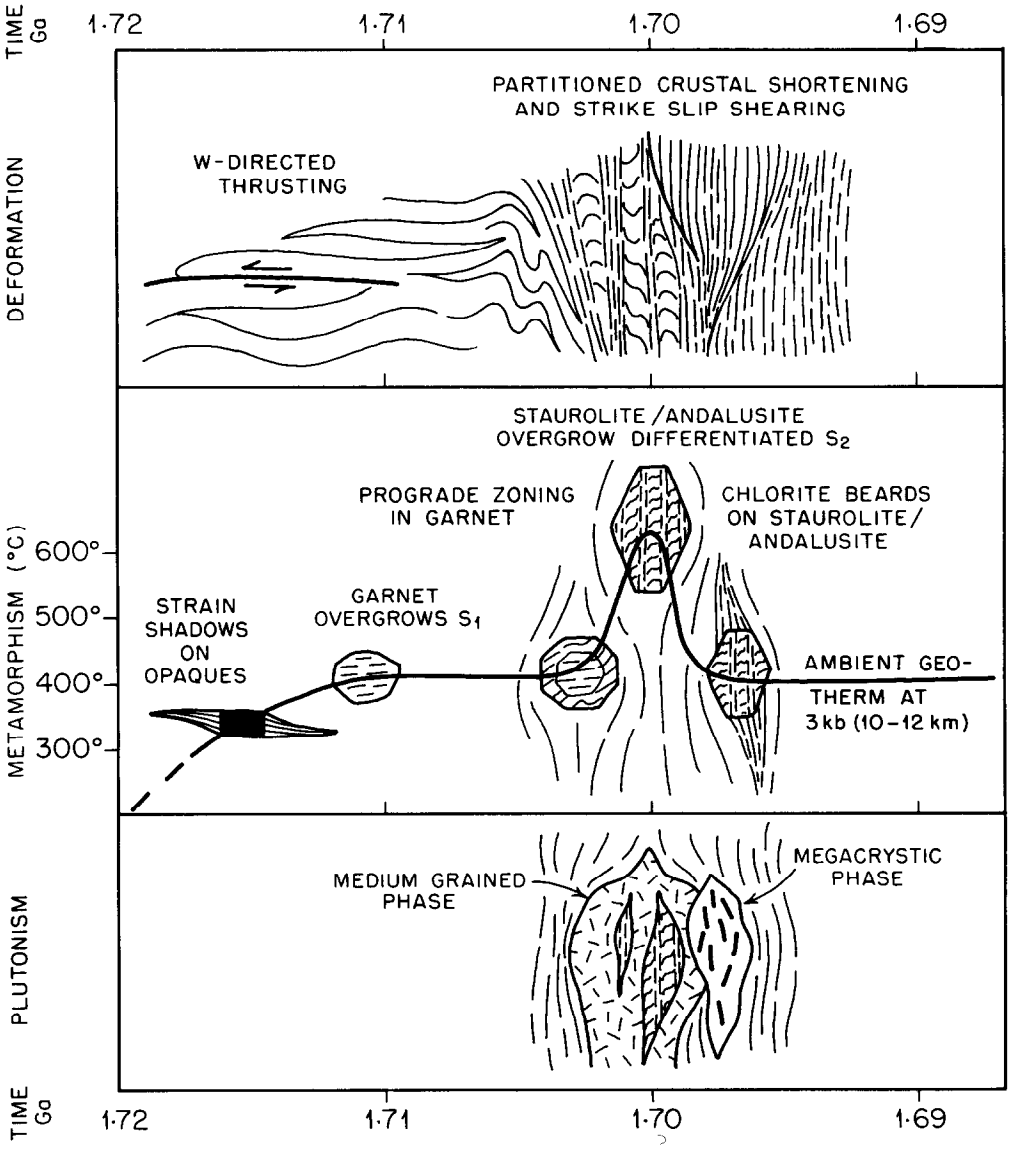

Fig. 16. Summary of porphyroblast timing relationships in the Crazy Basin area. Porphyroblasts document the progressive development of S_2 cleavage. Note that staurolite, and most of the garnet and biotite growth is interpreted to reflect heating from the Crazy Basin Monzogranite during crustal shortening.

phase equilibria and can be interpreted to be part of the prograde assemblage. Regardless of its habit or host phase, most chlorite is aligned parallel to the dominant S_2 fabric. This is interpreted to reflect the fact that shortening continued during and after the local metamorphic peak (i.e. heating associated with the Crazy Basin Monzogranite), and after the onset of retrograde metamorphic conditions. Thus, both prograde and retrograde chlorite was syntectonic, consistent with the interpretation that the metamorphic peak in the Crazy Basin area was short lived relative to the shortening event.

Fabric relationships for porphyroblasts in the Crazy Basin area are summarized in Fig. 16. These microstructures suggest that porphyroblast growth took place during crustal shortening and S_2 cleavage formation. Most garnet porphyroblasts appear to have grown early during the development of S_2 cleavage. Staurolite and andalusite grew at various stages during the development of the S_2 cleavage, with most crystals growing relatively late in the S_2 cleavage-forming event. This is compatible with the observation that these minerals formed by several metamorphic reactions. Chlorite is interpreted to be stable in most assemblages at the ambient regional metamorphic conditions (400–450°C, 3 kb), but is a retrograde phase in rocks near the Crazy Basin pluton because higher-grade conditions were a brief pluton-related thermal pulse in the ongoing tectono-metamorphic event.

SUMMARY AND DISCUSSION

Figure 17 and Table 1 summarize evidence for the synchroneity of deformation, plutonism and metamorphism in the Crazy Basin area. Individual criteria are commonly equivocal and our work suggests that apparent ambiguities in relative timing relationships are characteristic of syntectonic pluton emplacement. Table 1 includes alternate interpretations of individual lines of

Table 1. Summary, interpretation, and uncertainties of timing data. Numbers keyed to locations shown in Fig. 17

Observation	Syntectonic interpretation	Alternative interpretations based single line of evidence
Deformation and plutonism		
1 Main phase sills flattened and boudinaged around pluton margins	Shortening subperpendicular to pluton margins; stretching parallel to shallow NE lineation (related to Cleator shear zone); possible interaction of emplacement-related strains and regional deformation	Post-tectonic pluton—stretching above equatorial plane of a diapir (Lagarde *et al.* 1991); pre-tectonic pluton—deformation partitioning at pluton margins
2 Dike and vein arrays fill tension gashes	Extension shallow NNE; melts and pluton-related fluids present during sinistral shear related to Cleator shear zone	Post-tectonic pluton—emplacement-related shortening of granite veins perpendicular to margin of pluton but sinistral quartz vein arrays genetically unrelated to the pluton
3 Aplite dikes cross-cut composite S_1/S_2 cleavage but are folded by F_2 folds and contain S_2 cleavage	Aplites emplaced late during NW–SE shortening	Pre-tectonic pluton—aplites cross cut S_1 and were only weakly folded in a low F_2 strain domain that coincided with the hinge zone of a large scale F_1 antiform
4 Tabular pegmatites dikes strike NW and are subvertical	Orientation consistent with emplacement during NW–SE regional shortening	Post-tectonic pluton—pegmatite orientations related to NE–SW extension above the rising pluton
5 NE-trending foliation throughout the pluton	Reflects the incremental shortening direction during late stages of regional shortening	Pre-tectonic pluton—fabric represents the finite shortening strain in a competent pre-tectonic pluton
6 Parallel magmatic and solid state fabrics in the megacrystic phase, locally at a large angle to pluton margins	Phenocrysts aligned compatible with regional shortening and sinistral shear	Post-tectonic pluton—magmatic flow parallel to NE striking S_2 foliation
7 Screens and xenoliths contain S_1 and S_2 foliations; pluton contains S_2	Pluton post-dates much of NW–SE shortening	Pre-tectonic pluton—xenoliths may be more strongly foliated than their enclosing rocks due to competence contrasts
8 Xenoliths are aligned, long axes trend NE at NE margin of pluton	Xenoliths aligned perpendicular to regional shortening and sinistral shear	Pre-tectonic pluton—xenoliths record finite shortening; post-tectonic pluton—passive emplacement preserves NE alignment
9 Marginal foliation in granite parallel to marginal foliation in country rock	Interaction of regional and emplacement-related strains (Brun & Pons 1981)	Pre-tectonic pluton—deformation around an already crystallized pluton; post-tectonic pluton—strain related to forceful emplacement (Ramsay 1989)
10 Foliation triple point in country rock	Interaction of regional strain and emplacement-related strain (Brun & Pons 1981)	Pre-tectonic pluton—strain shadow around a pre-deformational pluton (Paterson *et al.* 1991)
Plutonism and metamorphism		
11 Isograds concentric with pluton; higher T mineral assemblages closer to pluton	Peak T assemblages reflect addition of heat from pluton to 400 °C ambient T at 10 km	Post-metamorphic pluton-emplaced into pre-pluton 'hot spot' (Chamberlain & Rumble 1990, Bradey 1990); pre-metamorphic pluton—basement effect—heat elevated in granite rock due to absence of dehydration reactions (Ayerton 1980, Morand 1988)
12 Quantitative thermobarometric data documents increasing T with constant P toward pluton	Peak metamorphic T synchronous with pluton emplacement	As above
13 Conductive thermal model of cooling pluton in 400 °C regional metamorphic terrane reproduces observed T conditions	Short-lived peak T conditions synchronous with pluton emplacement, 'pluton-enhanced regional metamorphism'	As above
Metamorphism and deformation		
14 Early porphyroblasts (gt,bt) overgrew S_1 and weak F_2 crenulations	Prograde porphyroblasts grew early during regional shortening	Porphyroblasts developed during F_1; weak crenulations in porphyroblasts due to rotation during F_1
15 Peak metamorphic porphyroblasts (and, st) overgrew well-developed S_2 fabric	Peak of thermal metamorphism occurred late during shortening	As above, complex inclusion fabrics reflect F_1 progressive deformation
16 Locally, peak metamorphic porphyroblasts (and, st) contain oblique internal foliation	(1) porphyroblast overgrew well-developed S_2 foliation which was then reoriented by progressive deformation; (2) porphyroblast overgrew crenulated S_1 fabric that was subsequently decrenulated in the matrix (Bell 1986)	Peak porphyroblasts may have undergone small amounts of rotation during F_2
17 Chlorite beards occur on peak metamorphic porphyroblasts	Beards represent a retrograde return to regional conditions after the pluton-induced heating, but during the later phase of shortening deformation	Chlorite beards may represent a later deformation (and metamorphism?) unrelated to the dominant matrix fabrics

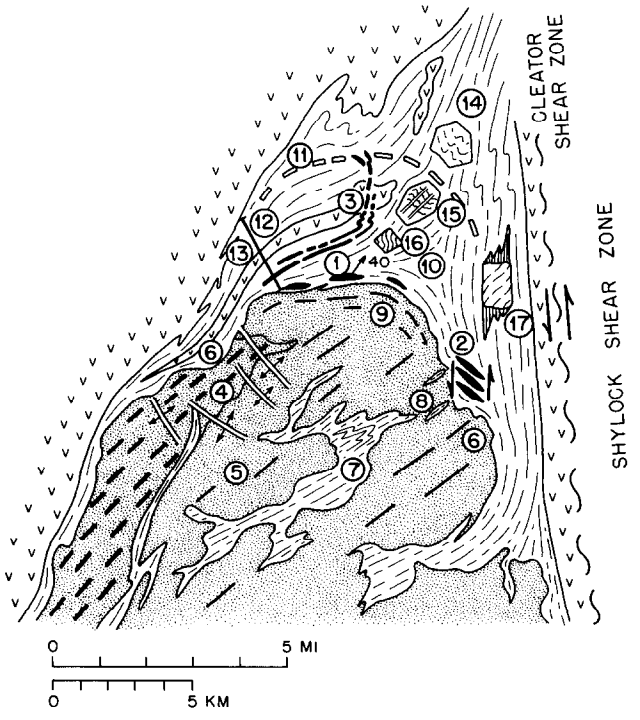

Fig. 17. Schematic summary of evidence for relative timing of pluton emplacement, regional deformation and metamorphism. Numbers keyed to Table 1.

evidence. However, the combined criteria are consistent with only a syn-shortening emplacement of the Crazy Basin Monzogranite. Deformational features in the pluton are more easily related to regional strains than emplacement related strains (1–8 of Table 1). Further, the association of peak metamorphic porphyroblasts with both heat of emplacement (11–13 of Table 1) and syn-shortening microstructures in prograde (14–16 of Table 1) and retrograde (17 of Table 1) porphyroblasts indicate synchronous deformation, metamorphism and plutonism.

In evaluating the evidence for syntectonic emplacement, it is useful to consider the strengths and weaknesses of the alternative arguments for either a pre- or a post-tectonic emplacement model. While the pluton certainly post-dated appreciable deformation (1, 7 of Table 1), and contains fabrics that may be related to emplacement (4, 9, 10 of Table 1), an entirely post-tectonic interpretation for the Crazy Basin Monzogranite requires that all of the deformational features in the granite, in related injections, and pluton-parallel foliations in the country rocks adjacent to the pluton formed in response to emplacement-related strains (e.g. Bateman 1985, Courrioux 1987, Ramsay 1989). This seems unlikely in view of similar kinematic regimes for pluton and country rock fabrics (2, 3, 5 of Table 1) and the parallelism of magmatic and solid state deformational fabrics (6 of Table 1) within the pluton. A post-tectonic interpretation also has difficulty explaining the observed syn-deformational porphyroblasts and the thermal high centered on the pluton.

A pretectonic interpretation for the pluton can explain similar kinematic frameworks inside and outside of the pluton, and might attribute differences in fabric intensity from pluton to country rock to deformation partitioning. However, we see no good explanation in such a model for the cross cutting aplite (1 of Table 1), the NW-trending pegmatites (3 of Table 1), parallel magmatic and solid state fabrics (6 of Table 1), and strongly deformed xenoliths within weakly deformed granite (7 of Table 1). The distribution of metamorphic assemblages might be attributed to a 'basement effect', (Fonteilles & Guitard 1968, Ayerton 1980) where granite rock remained hot during post-emplacement regional metamorphism while cover rocks cooled by dehydration reactions (Morand 1988). However, no similar 'basement effect' is observed around pre-tectonic 1.74–1.72 Ga plutons elsewhere in the Big Bug block, such as the Brady Butte and Crooks Canyon granodiorites, and calculated temperatures of 630 °C would seem to require a substantial magmatic heat input at these shallow crustal levels.

Implication for mode emplacement of the Crazy Basin Monzogranite

Our syntectonic interpretation for emplacement of the Crazy Basin Monzogranite has implications for understanding mechanisms of pluton emplacement. The geometry of sheetlike NE-striking dikes and abundant screens and xenoliths in the central and southern parts of the pluton suggest magma ascent and emplacement as sheets along fractures and conduits whose geometry was influenced by pre-existing anisotropy. A predominantly passive emplacement of the pluton (i.e. where magma is responding to rather than generating deforming stresses) is supported by the similarity of strains in screens and distant country rock. However, the marginal foliation in the granite and country rock in the northern margin suggests either stresses generated by pluton emplacement and/or modification of regional stresses along the pluton's margins.

Passive syntectonic emplacement has been documented in extensional and tranpressional regimes (e.g. Hutton 1982, 1988a,b, Castro 1986, Guineberteau *et al.* 1987). In contractional regimes, however, magma ascent and emplacement in foliation-parallel screens may be inhibited by normal stress acting across foliation planes. Such emplacement, as at Crazy Basin, would seem to require that normal stresses across foliation were exceeded by magma pressure. Tobisch & Paterson (1990) and Paterson (1989) have proposed that plutons can be intradeformational, where compressive stresses are relaxed periodically allowing ascent of magma. Alternatively, it may be that late syntectonic emplacement reflects the waning of contractional deformation and the ability of magma pressure to exceed compressive forces (Karlstrom 1989b). However, neither of these models adequately explains the syn-pluton, syn-deformational porphyroblasts and the participation of melt in regional deformation in the Crazy Basin pluton.

Emplacement of the Crazy Basin Monzogranite dur-

ing bulk crustal shortening was apparently associated with temporal partitioning of deformation. Darrach *et al.* (1991) suggested that regional shortening was spatially and temporally partitioned into zones of shortening and sinistral strike slip during pluton emplacement, with strike slip generally overprinting shortening. We suggest that partitioning of convergent deformation into dominantly strike-slip conjugate zones such as the Cleator and Chaparral shear zones would reduce, perhaps periodically, normal stress in intervening blocks sufficiently to allow emplacement. This would better explain the parallelism of the lineation in the margin of the pluton with the extension direction in Cleator shear zone. Likewise, the late-shortening timing of emplacement is compatible with the interpretation that early homogeneous shortening by folding and foliation development gave way (with temporal overlap) to more inhomogeneous bulk shortening by escape-block movement along conjugate shear zones.

This model suggests that granite was emplaced in sheets parallel to the existing NE-striking shortening foliation during times of strike-slip-dominated deformation. This is consistent with the position of the pluton towards the southern end of the SW-escaping Big Bug block (Fig. 4). Dilation associated with accumulation of magma here was synchronous with southwestward escape and inhomogeneous shortening of the Big Bug block. Emplacement of NE-striking sheets may have been facilitated by tensional bridges that developed between *P*-shears during sinistral slip, as proposed by Tikoff & Teyssier (1992). Thus our model is compatible with models proposed by numerous workers for emplacement of arc batholiths during active shearing along major transpressional boundaries (Hutton 1988, Miller & Bowring 1990, D'Lemos *et al.* 1992, Hutton & Reavy 1992, Tikoff & Teyssier 1992). The decoupling of normal and strike-slip components of oblique convergence may be a common feature of convergent zones at all scales (Fitch 1972, Kirby 1991), and may be a major control of granitoid ascent and emplacement.

Implications for durations of orogenic processes

One of the most difficult aspects of understanding interaction of orogenic processes is an evaluation of rates and durations of tectonic processes and events (Paterson & Tobisch 1992). Figure 16 shows our interpretation of duration of events in the Crazy Basin area. Rates associated with magma ascent and final crystallization are generally believed to be quite fast (Paterson & Tobisch 1992), 10^3–10^5 years for moderate size plutons (less than 200 km^3) like the Crazy Basin Monzogranite. Ascent of this much magma along conduits and fractures, as is suggested by the sheeted character of much of the pluton, could have taken 10^3–10^5 y (Shaw 1985, Paterson & Tobisch 1992). Cooling of the pluton to the ambient temperature of the country rock may have taken as much as 10^6 y (Fig. 13), but crystallization through the critical melt fraction (van der Molen & Paterson 1979) and the accompanying sharp change from magmatic to solid state flow would have been much faster, about 10^3–10^5 y, because of the limited thermal budget of crystallizing plutons (Miller *et al.* 1990). Growth of metamorphic porphyroblasts may also take place in 10^3–10^5 y (Bell & Cuff 1989, Paterson & Tobisch 1992, Williams 1994), especially associated with contact metamorphism (Joesten & Fischer 1988). Thus, while the prograde path of regional metamorphism probably took place over longer periods of time (10^6–10^7 y) and the retrograde path may have involved slow cooling over 10^8 y (Hodges *et al.* 1994), our data suggest that peak metamorphic conditions may have been locked during a brief thermal pulse whose duration coincided with the duration of pluton emplacement. In areas that experienced pluton-enhanced metamorphism, initial retrograde metamorphism (return to regional ambient conditions) apparently overlapped with deformation over time spans of less than 10^6 y and more effective retrogression may have been facilitated in zones of high fluid flux like the Shylock shear zone.

Duration of deformation was probably longer. In contractional settings, lithospheric plates collide over 10^6–10^8 y and collision of individual arcs, seamounts, or oceanic plateaus at convergent margins may last 10^6–10^7 y (Hamilton 1988). Timing of deformation data in central Arizona (Karlstrom & Bowring 1991) suggest that early recumbent folding in the Big Bug block may have started as early as 1.72 Ga and NW–SE shortening started before and continued beyond 1.70 Ga (Fig. 16). Development of cleavages and the associated >50–100% shortening in the Crazy Basin area might have taken 10^6 years at time-averaged orogenic strain rates of 10^{-14} s^{-1} (Pfiffner & Ramsay 1982). However, since inclusion trails within syn-pluton porphyroblasts record various stages in the development of the shortening fabric, we suggest that heat from the pluton punctuated deformation and increased local strain rates such that much of the observed shortening took place during the $<10^5$ years associated with rapid cooling of the pluton and its aureole. This is consistent with pluton-enhanced rapid strain rates postulated for other syn-contractional plutons (Karlstrom *et al.* 1993).

Several points of general interest emerge from this model. Rates of diffusion and deformation were locally dramatically increased due to a brief rise in temperature. Thus, fabrics and metamorphic assemblages, through part of a regional continuum, can develop diachronously and rapidly. This style of pluton-enhanced regional deformation and metamorphism apparently characterizes the Early Proterozoic tectonic evolution of central Arizona (Karlstrom & Bowring 1991, Williams 1991), and may characterize many high *T*-low *P* metamorphic belts.

Acknowledgements—This paper benefitted from the detailed mapping of Dean Argenbright, Marc Darrach, structural geology classes at Northern Arizona University, and undergraduate students Britt Callahan and Brad Ball. Research was supported by NSF grants Ear-8411998-02, Ear-8707746, and Ear-8916494, to KEK, S. A. Bowring, and MLW, and by donors to the Petroleum Research Fund of the

American Chemical Society (PRF-16199-GB2). Discussions with S. A. Bowring, T. Hoisch and J. L. Burr added significantly to this research and are much appreciated. We thank Tim Allen, Ian Dalziel and Steve Wojtal for helpful reviews of the paper.

REFERENCES

Allen, T. & Chamberlain, C. P. 1989. Thermal consequences of mantled gneiss dome emplacement. *Earth Planet. Sci. Lett.* **93**, 392–404.

Anderson, C. A. & Blacet, P. M. 1972. Precambrian geology of the northern Bradshaw Mountains, Yavapai County, Arizona. *Bull. U.S. geol. Surv.* **1336**.

Anderson, C. A., Blacet, M. P., Silver, L. T. & Stern, T. W. 1971. Revision of Precambrian stratigraphy in the Prescott–Jerome area, Yavapai County, Arizona. *Bull. U.S. geol. Surv.* **1324-6**, 1–16.

Anderson, P. 1989. Stratigraphic framework, volcanic-pluton evolution, and vertical deformation of the Proterozoic volcanic belts of central Arizona. In: *Geologic Evolution of Arizona* (edited by Jenney, J. P. & Reynolds, S. J.). *Ariz. geol. Soc. Dig.* **17**, 57–148.

Ayerton, S. 1980. High fluid pressure, isothermal surfaces, and the initiation of nappe movement. *Geology* **8**, 172–174.

Barton, M. D. & Hanson, R. B. 1989. Magmatism and the development of low-pressure metamorphic belts: implications from the western United States and thermal modeling. *Bull. geol. Soc. Am.* **101**, 1051–1065.

Bateman, R. 1984. On the role of diapirism in the segregation, ascent, and final emplacement of granitoid magmas. *Tectonophysics* **110**, 211–231.

Bateman, R. 1985. Aureole deformation by flattening around a diapir during *in situ* ballooning: the Cannibal Creek granite. *J. Geol.* **93**, 293–310.

Bell, T. H. 1981. Foliation development—the contribution, geometry and significance of progressive, bulk, inhomogeneous shortening. *Tectonophysics* **75**, 273–296.

Bell, T. H. 1986. Foliation development and refraction in metamorphic rocks: reactivation of earlier foliations and decrenulation due to shifting patterns of deformation partitioning. *J. Meta. Geol.* **4**, 421–444.

Bell, T. H. & Cuff, C. 1989. Dissolution, solution transfer, diffusion versus fluid flow and volume loss during deformation/metamorphism. *J. Meta. Geol.* **7**, 425–447.

Bell, T. H. & Hayward, N. 1991. Episodic metamorphic reactions during orogenesis: the control of deformation partitioning on reaction sites and reaction duration. *J. Meta. Geol.* **9**, 619–640.

Bell, T. H. & Johnson, S. E. 1989. Porphyroblast inclusion trails: the key to orogenesis. *J. Meta. Geol.* **7**, 151–168.

Bell, T. H. & Rubenach, M. J. 1983. Sequential porphyroblast growth and crenulation cleavage development during progressive deformation. *Tectonophysics* **92**, 171–194.

Bell, T. H., Fleming, P. D. & Rubenach, M. J. 1986. Porphyroblast nucleation, growth and dissolution in regional metamorphic rocks as a function of deformation partitioning during foliation development. *J. Meta. Geol.* **4**, 37–67.

Bennett, V. C. & DePaolo, D. J. 1987. Proterozoic crustal history of the western United States as documented by neodymium isotopic mapping. *Bull. geol. Soc. Am.* **99**, 674–685.

Bergh, S. G. & Karlstrom, K. E. 1992. The Chaparral fault zone of central Arizona: deformation partitioning and escape block tectonics during Proterozoic orogeny. *Bull. geol. Soc. Am.* **104**, 329–345.

Blacet, P. M. 1966. Unconformity between gneissic granodiorite and overlaying Yavapai Series (older Precambrian), central Arizona. *Prof. Pap. U.S. geol. Surv.* **550-B**, 1–5.

Blacet, P. M. 1968. Precambrian geology of the southwest quarter of the Mount Union Quadrangle, Bradshaw Mountains, central Arizona. Unpublished Ph.D. thesis, Stanford University.

Blacet, P. M. 1985. Proterozoic geology of the Brady Butte area, Yavapai County, Arizona. *Bull. U.S. geol. Surv.* **1548**, 55.

Blumenfeld, P. & Bouchez, J. L. 1988. Shear criteria in granite and migmatite deformed in the magmatic and solid states. *J. Struct. Geol.* **10**, 361–372.

Bowring, S. A. & Karlstrom, K. E. 1990. Growth, stabilization, and reactivation of Proterozoic lithosphere in the southwestern United States. *Geology* **18**, 1203–1206.

Brady, J. B. 1988. The role of volatiles in the thermal history of metamorphic terranes. *J. Petrol.* **29**(6), 1187–1213.

Brun, J. P. & Pons, J. 1981. Strain patterns of pluton emplacement in a crust undergoing non-coaxial deformation, Sierra Morena, southern Spain. *J. Struct. Geol.* **3**, 219–229.

Burr, J. L. 1991. Proterozoic stratigraphy and structural geology of the Hieroglyphic Mountains, central Arizona. *Spec. Pap. geol. Soc. Ariz.* **19**, 117–134.

Burr, J. L. 1992. Early Proterozoic structural geology, metamorphism, and effects of pluton emplacement, southern Big Bug tectonic block, Hieroglyphic Mountains, central Arizona. Unpublished Ph.D. thesis, University of Massachusetts, Amherst.

Castro, A. 1986. Structural pattern and ascent model in the eastern Extremadura batholith, Hercynian belt, Spain. *J. Struct. Geol.* **8**, 633–645.

Chamberlain, C. P. & Rumble, D. I. 1989. Thermal anomalies in a regional metamorphic terrane: an isotopic study of the role of fluids. *J. Petrol.* **29**(6), 1215–1232.

Chamberlain, K. & Bowring, S. A. 1990. U–Pb geochronology of Proterozoic rocks in northwestern Arizona: implication for crustal growth. *J. Geol.* **98**, 399–416.

Collins, W. J. & Vernon, R. H. 1991. Orogeny associated with anti clockwise *P–T–t* paths: evidence from low-*P*, high-*T* metamorphic terranes in the Arunta inlyer, central Australia. *Geology* **19**, 835–838.

Conway, C. M., Karlstrom, K. E., Silver, L. T. & Wrucke, C. T. 1987. Tectonic and magmatic contrasts across a two-province Proterozoic boundary in central Arizona. In: *Geologic Diversity of Arizona and its Margins* (edited by Davis, G. H. & VandenDolder, E. M.). Excursions to choice areas. *Spec. Pap. Ariz. Bur. Miner. Tech.* **5**, 158–175.

Courrioux, G. 1987. Oblique diapirism: the Criffel granodiorite/granite zoned pluton (southwest Scotland). *J. Struct. Geol.* **9**, 313–330.

Darrach, M. E., Karlstrom, K. E., Williams, M. L. & Argenbright, D. N. 1991. Progressive deformation in the Early Proterozoic Shylock shear zone, central Arizona. In: *Early Proterozoic Geology and Ore Deposits of Arizona* (edited by Karlstrom, K. E.). *Ariz. geol. Soc. Dig.* **19**, 97–116.

D'Lemos, R. S., Brown, M. & Strackan, R. A. 1992. Granite magma generation, ascent, and emplacement within a transpressional orogen. *J. geol. Soc. Lond.* **149**, 482–490.

den Tex, E. 1963. A commentary on the correlation of metamorphism and deformation in space and time. *Geologie Mijnb.* **42**, 170–176.

DeWitt, E. 1976. Precambrian geology and ore deposits of the Mayer-Crown King area, Yavapai County, Arizona. Unpublished M.S. thesis, University of Arizona.

DeWitt, E. 1989. Geochemistry and tectonic polarity of Early Proterozoic (1700–1750 Ma) plutonic rocks, north-central Arizona. In: *Geologic Evolution of Arizona* (edited by Jenny, J. P. and Reynolds, S. J.). *Ariz. geol. Soc. Dig.* **17**, 149–164.

DePaolo, D. J. 1981. Neodymium isotopes in the Colorado Front Range and crust-mantle evolution in the Proterozoic. *Nature* **271**, 193–196.

Ferry, J. M. & Spear, F. S. 1978. Experimental calibration of the partitioning of Fe and Mg between biotite and garnet. *Contrib. Mineral. Petrol.* **66**, 113–117.

Fitch, T. J. 1972. Plate convergence, transcurrent faults and internal deformation adjacent to southeast Asia and western Pacific. *J. geophys. Res.* **77**, 4432–4460.

Fonteilles, M. & Guitard, G. 1968. L'effet de socle dans le metamorphism. *Bull. Soc., fr. Minér. Cristallogr.* **91**, 185–206.

Gapais, D. 1989. Shear structures within deformed granites: mechanical and thermal indicators. *Geology* **17**, 1144–1147.

Ghent, E. D. & Stout, M. Z. 1981. Geobarometry and geothermometry of plagioclase–biotite–garnet–muscovite assemblages. *Contrib. Mineral. Petrol.* **76**, 92–97.

Grambling, J. A. & Ward, D. B. 1987. Thrusting of the Pecos greenstone belt over younger supracrustal rocks, Rio Mora area, New Mexico. *Geol. Soc. Am. Abstr. w. Prog.* **19**, 278.

Gromet, L. P. 1991. Direct dating of deformational fabrics. *Mineral. Ass. Canada Short Course Notes*. Toronto, Canada.

Guineberteau, B., Bouchez, J. L. & Vigneresse, J. L. 1987. The Mortagne granite pluton (France) emplaced by pull apart along a shear zone: structural and gravimetric arguments and regional implications. *Bull. geol. Soc. Am.* **99**, 763–770.

Hamilton, W. B. 1988. Plate tectonics and island arcs. *Bull. geol. Soc. Am.* **100**, 1503–1527.

Hodges, K. V. & Crowley, P. D. 1985. Error estimation and empirical geothermobarometry for pelitic systems. *Am. Miner.* **72**, 671–680.

Hodges, K. V., Hames, W. E. & Bowring, S. A. 1994. $^{40}Ar/^{39}Ar$ age gradients in micas from a very high temperature–low pressure

metamorphic terrane: evidence for very slow cooling and implications for the interpretation of age spectra. *Geology* **22**, 55–58.
Hoffman, P. F. 1988. United Plates of America: birth of a craton. *Annu. Rev. Earth & Planet. Sci.* **16**, 543–603.
Hoisch, T. D. 1990. Empirical calibration of six geobarometers for the mineral assemblage quartz + muscovite + biotite + plagioclase + garnet. *Contrib. Mineral., Petrol.* **104**, 225–234.
Hutton, D. H. W. 1982. A tectonic model for emplacement of the Main Donegal granite, NW Ireland. *J. geol. Soc. Lond.* **139**, 615–631.
Hutton, D. H. W. 1988a. Granite emplacement mechanism and tectonic controls: inferences from deformation studies. *Trans. R. Soc. Edinb.* **79**, 245–255.
Hutton, D. H. W. 1988b. Igneous emplacement in shear zone: the biotite granite at Strontian, Scotland. *Bull. geol. Soc. Am.* **100**, 1392–1399.
Hutton, D. H. W. & Reavy, R. S. 1992. Strike-slip tectonics and granite petrogenesis. *Tectonophysics*.
Jagger, T. A. & Palache, C. 1905. Description of the Bradshaw Mountains Quadrangle. *U.S. geol. Surv.* Atlas, Folio 126, 16.
Jerome, S. E. 1956. Reconnaissance study of the Black Canyon schist belt, Bradshaw Mountains, Yavapai and Maricopa counties, Arizona. Unpublished Ph.D. thesis, University of Utah.
Joesten, R. & Fisher, G. 1988. Kinetics of diffusion-controlled mineral growth in the Christmas Mountains (Texas) contact aureole. *Bull. geol. Soc. Am.* **100**, 714–732.
Karlstrom, K. E. 1989a. Early recumbent folding during Proterozoic orogeny in central Arizona. *Spec. Pap. geol. Soc. Am.* **235**, 155–172.
Karlstrom, K. E. 1989b. Towards a syntectonic paradigm for granites. *Eos.* **70**, 762–770.
Karlstrom, K. E. & Argenbright, D. N. 1985. Structural evidence for syntectonic intrusion of the Crazy Basin Quartz Monzonite, central Arizona. *Geol. Soc. Am. Abstr. w. Prog.* **17**, 228.
Karlstrom, K. E. & Bowring, S. A. 1988. Early Proterozoic assembly of tectonostratigraphic terranes in southwestern North America. *J. Geol.* **96**, 561–576.
Karlstrom, K. E. & Bowring, S. A. 1991. Styles and timing of Early Proterozoic deformation in Arizona. In: *Proterozoic Geology and Ore Deposits of Arizona* (edited by Karlstrom, K. E.). *Ariz. geol. Soc. Dig.* **19**, 1–10.
Karlstrom, K. E. & Bowring, S. A. 1993. Proterozoic orogenic history in Arizona. In: *Transcontinental Proterozoic Provinces, chapter* 4: *The Geology of North America* (edited by Van Schmus, W. R. & Bickford. M. E.), v. C-2: Precambrian of the Conterminous U.S. The Geological Society of America (DNAG).
Karlstrom, K. E., Bowring, S. A. & Conway, C. M. 1987. Tectonic significance of an Early Proterozoic two-province boundary in central Arizona. *Bull. geol. Soc. Am.* **99**, 529–538.
Karlstrom, K. E. & Conway, C. M. 1986. Deformational styles and contrasting lithostratigraphic sequences with an Early Proterozoic orogenic belt, central Arizona. In: *Geology of Central and Northern Arizona* (edited by Nations, J. D., Conway, C. M. & Swann, G. A.). Geol. Soc. Am. Rocky Mountain Section Guidebook. Flagstaff, AZ. 1-26.
Karlstrom, K. E., Miller, C. F., Kingsbury, J. A. & Wooden, J. L. 1993. Pluton emplacement along an active ductile thrust zone, Piute Mountains, southeastern California: interaction between deformational and solidification processes. *Bull. geol. Soc. Am.* **105**, 213–130.
Kortemeier, C. P. 1984. Geology of the tip top district, Yavapai County, Arizona. Unpublished M.S. thesis, Arizona State University, Tempe.
Kirby, S. H. 1991. *Tectonophysics* 1987–1990. *Rev. Geophys. Suppl.* 743–747.
Lagarde, J. L., Omar, S. A. & Roddaz, B. 1991. Structural characteristics of granitic plutons emplaced during weak regional deformation: examples from late Carboniferous plutons, Morocco. *J. Struct. Geol.* **12**, 805–821.
Leighty, Robert, Best, D. M. & Karlstrom, K. E. 1991. Gravity and magnetic evidence for a Proterozoic crustal boundary along the southern Shylock shear zone, central Arizona. In: *Proterozoic Geology and Ore Deposits of Arizona* (edited by Karlstrom, K. E.). *Ariz. geol. Soc. Dig.* **19**, 135–152.
Lux, D. R., DeYoreo, J. J., Guidotti, C. V. & Decker, E. R. 1986. Role of plutonism in low pressure metamorphic belt formation. *Nature* **323**, 794–797.
McDougal, I. & Harrison, T. M. 1988. *Geochronology and Thermochronology by the* $^{40}Ar/^{39}Ar$ *Method*. Oxford University Press, New York.
Mezger, K., Rawnsley, C. M., Bohlen, S. R. & Hanson, G. N. 1991. U–Pb garnet, sphene, monazite, and rutile ages: implications for the duration of high-grade metamorphism and cooling histories, Adirondack Mts., New York. *J. Geol.* **99**, 415–428.
Miller, C. F., Watson, E. B. & Harrison, T. M. 1990. Perspectives on the source, segregation, and transport of granitoid magmas. *Trans. R. Soc. Edinb.* **79**, 135–156.
Miller, R. B. & Bowring, S. A. 1990. Structure and chronology of the Oval Peak batholith and adjacent rocks: implications for the Ross Lake fault zone, North Cascades, Washington. *Bull. geol. Soc. Am.* **102**, 1361–1377.
Morand, V. J. 1988. Emplacement and deformation of the Wyangala Batholith, New South Wales. *J. Earth Sci. Austr.* **35**, 339–353.
O'Hara, P. F. 1980. Metamorphic and structural geology of the Northern Bradshaw Mountains, Yavapai County, Arizona. Unpublished Ph.D. thesis, Arizona State University.
Page, R. W. & Bell, T. H. 1985. Isotopic and structural responses of granite to successive deformation and metamorphism. *J. Geol.* **94**, 365–379.
Paterson, S. R. 1989. Are syntectonic granites truly syntectonic (?). *Eos.* **70**, 763–770.
Paterson, S. R., Brudos, T., Fowler, K., Carlson, C., Bishop, K. & Vernon, R. H. 1991. Papoose Flat pluton: forceful expansion or post-emplacement deformation? *Geology* **19**, 324–327.
Paterson, S. R. & Tobisch, O. T. 1988. Using pluton ages to date regional deformations: problems with commonly used criteria. *Geology* **16**, 1108–1111.
Paterson, S. R. & Tobisch, O. T. 1992. Rates of geological processes in magmatic arcs: implications for the timing and nature of pluton emplacement and wall rock deformation. *J. Struct. Geol.* **14**, 291–300.
Paterson, S. R., Vernon, R. H. & Fowler, Jr. K. 1991. Aureole tectonics. In: *Contact Metamorphism* (edited by Kerrick, D. M.). *Mineral. Soc., Am. Rev. Mineral.* **26**, 673–722.
Paterson, S. R., Vernon, R. H. & Tobisch, O. T. 1989. A review of criteria for the identification of magmatic and solid state foliations in granitoids. *J. Struct. Geol.* **11**, 349–363.
Pattison, D. R. M. & Tracy, R. J. 1991. Phase equilibria and thermobarometry of metapelites. In: *Contact Metamorphism* (edited by Kerrick, D. M). *Rev. Mineral.* **26**, 105–206.
Philpotts, A. R. 1990. *Principles of Igneous and Metamorphic Petrology*. Prentice-Hall, Englewood Cliffs, New Jersey.
Pfiffner, O. A. & Ramsay, J. G. 1982. Constraints on geologic strain rates: arguments from finite strain states of naturally deformed rocks. *J. geophys. Res.* **87**, 311–321.
Ramsay, J. G. 1989. Emplacement kinematics of a granite diapir: the Chindamora batholith, Zimbabwe. *J. Struct. Geol.* **11**, 191–210.
Shafiqullah, M., Damon, P. E., Lynch, D. J., Reynolds, S. J., Rehrig, W. A. & Raymond, R. H. 1980. K–Ar geochronology and geologic history of southwestern Arizona and adjacent areas. In: *Studies in Western Arizona* (edited by Jenny, J. P. & Stone, C.). *Ariz. geol. Soc. Dig.* **12**, 201–260.
Shaw, H. R. 1985. Links between magma–tectonic rate balances, plutonism, and volcanism. *J. geophys. Res.* **90**, 11,275–11,288.
Simpson, C. 1985. Deformation of granitic rocks across the brittle–ductile transition. *J. Struct. Geol.* **7**, 503–511.
Simpson, C. & DePoar, D. 1991. Deformation and kinematics of high strain zones, 1991 Annual GSA meeting—San Diego, Short Course Notes.
Simpson, C. & Winch, R. P. 1986. Evidence for deformation-induced K-feldspar replacement by myrmekite. *J. Meta. Geol.* **7**, 261–275.
Spear, F. S., Ferry, J. M. & Rumble, D. 1982. Analytical formulation of phase equilibria: the Gibbs method. In: *Characterization of Metamorphism through Mineral Equilibria* (edited by Ferry, J. M.). *Mineral. Soc. Am. Rev. Mineral.* **10**, 105–152.
Spear, F. S. & Peacock, S. M. 1989. Metamorphic pressure–temperature–time paths. *Am. Geophy. Un. Short Course in Geology* **7**, 102.
Streikeissen, 1976. To each plutonic rock its proper name. *Earth Sci. Rev.* **12**, 1–33.
Symmes, G. H. & Ferry, J. M. 1992. The effect of whole-rock MnO content on the stability of garnet in pelitic schists during metamorphism. *J. Meta. Geol.* **10**, 221–238.
Tikoff, B. & Teyssier, C. 1992. Crustal-scale, en-échelon "*P*-shear" tensional bridges: a possible solution to the batholithic room problem. *Geology* **20**, 927–930.
Tobisch, O. T. & Paterson, S. R. 1990. The Yarra granite. An intradeformational pluton associated with ductile thrusting, Lachlan Fold Belt, southeastern Australia. *Bull. geol. Soc. Am.* **102**, 693–703.

Turcotte, D. L. & Schubert, G. 1982. *Geodynamics Applications of Continuum Physics to Geological Problems*. John Wiley & Sons, New York.

Tullis, J. 1983. Deformation of feldspars. In: *Feldspar Mineralogy* (edited by Ribbe, P. H.). *Mineral. Soc. Am.* Short Course Notes 2, 297–323.

van der Molen, I. & Paterson, M. S. 1979. Experimental deformation of partially-melted granite. *Contrib. Mineral. Petrol.* **70**, 299–318.

Vance. R. K. 1989. Geochemistry and tectonic setting of the Yavapai Supergroup, west central Arizona. Unpublished Ph.D. thesis, New Mexico Institute of Mining and Technology, Socorro, New Mexico.

Vernon, R. H. 1989. Porphyroblast-matrix microstructural relationships: recent approaches and problems. In: *Evolution of Metamorphic Belts* (edited by Daly, J. S., Cliff, R. A. & Yardley, B. W. D.). Blackwell Scientific Publications, Oxford.

Vernon, R. H. & Flood, R. H. 1988. Contrasting deformation of *S*- and *I*-type granitoids in the Lachlan Fold Belt, eastern Australia. *Tectonophysics* **147**, 127–144.

Wickham, S. M. 1987. The segregation and emplacement of granitic magmas. *J. geol. Soc. Lond.* **144**, 281–297.

Williams, M. L. 1991. Overview of Early Proterozoic metamorphism in Arizona. In: *Proterozoic Geology and Ore Deposits of Arizona* (edited by Karlstrom, K. E.). *Ariz. geol. Soc. Dig.* **19**, 11–26.

Williams, M. L. 1994. Sigmoidal inclusion trails, punctuated fabric development, and interactions between metamorphism and deformation. *J. Meta. Geol.* **12**, 1–21.

Williams, M. L. & Grambling, J. A. 1990. Manganese, ferric iron, and the equilibrium between garnet and biotite. *Am. Miner.* **75** (7–8), 886–908.

Williams, M. L. & Karlstrom, K. E. 1990. Synchronous metamorphism, deformation, and plutonism in Proterozoic rocks of central Arizona. *Geol. Soc. Am. Abstr. w. Prog.* **22** (3), 94.

Wintsch, R. P. 1985. The possible effects of deformation on chemical processes in metamorphic fault zones. In: *Advances in Physical Geochemistry* (edited by Saxena, S. K.). Springer-Verlag, New York, 251–268.

Yardley, B. W. D., Barker, J. J. & Gray, J. R. 1987. The metamorphism of the Dalradian rocks of western Ireland and its relation to tectonic setting. *Phil. Trans. R. Soc. Lond.* **A321**, 243–268.

Zeitler, P. K. 1989. The geochronology of metamorphic processes. In: *Evolution of Metamorphic Belts* (edited by Daly, O. J. S., Cliff, R. A. & Yardley, B. W. D.). Blackwell Scientific Publications, Oxford.